Mechanism and Machine Theory 214 (2025) 106090

Contents lists available at ScienceDirect

Mechanism and Machine Theory

journal homepage: www.elsevier.com/locate/mechmt

Research paper

Dynamic model of multi-DOF spherical mechanisms based on instantaneous pole axes

Raffaele Di Gregorio

Department of Engineering, University of Ferrara Via Saragat,1, 44122 Ferrara, Italy

ARTICLE INFO

Keywords:
Dynamics
Spherical Mechanisms
Instantaneous Pole Axis
Velocity-Coefficient Vector
Acceleration-Coefficient Jacobian

ABSTRACT

Spherical mechanisms have the peculiarity that a point (spherical motion center (SMC)) is at rest with respect to all the links. This feature makes the links perform only rotations around axes (instantaneous pole axes (IPAs)) passing through the SMC. IPAs' locations fully describe their instantaneous kinematics and, in single-DOF mechanisms, uniquely depend on the mechanism configuration. In multi-DOF spherical mechanisms, IPAs' locations are determinable by considering the single-DOF mechanisms generated from the multi-DOF ones by locking all the actuated joints but one. Exhaustive analytic/geometric techniques that determine all the IPAs' locations of single-DOF spherical mechanisms by using only their configuration data are present in the literature. Here, a dynamic model of multi-DOF spherical mechanisms, which is general and strictly relates dynamic behavior and IPAs' locations, is deduced by exploiting these results. This novel model can consider also possible frame motions. The proposed formulation lends itself better than others to satisfy dynamic requirements during mechanism design. Eventually, a relevant case study illustrates its effectiveness.

1. Introduction

Spherical mechanisms are, by definition, those where all the links perform only instantaneous rotations around axes (Instantaneous Pole Axes (IPAs)) that pass through a point (spherical motion center (SMC)), which is shared by all the links [1]. Consequently, the SMC is a point at rest with respect to all the links, and the links can change only their relative orientation. Such a motion type (spherical motion) enters in many applications (see [2–12], for instance) where orientating a rigid body is the task to accomplish and an ample literature (see [1,10–24], for instance) addresses kinematic and/or dynamic problems of spherical mechanisms.

IPAs' locations, which are uniquely determined by their directions, fully describe instantaneous kinematics of spherical mechanisms [25]. In single-degree-of-freedom (single-DOF) spherical mechanisms, they uniquely depend on the mechanism configuration [26]. Differently, in multi-DOF spherical mechanisms, IPAs' directions are determinable by considering the single-DOF mechanisms generated from the multi-DOF one by locking all the actuated joints but one [25]. Exhaustive analytic and geometric techniques that determine all the IPAs' directions of single-DOF spherical mechanisms by using only their configuration data are present in the literature (see [26,27], for instance).

Due to the duality between instantaneous kinematics and statics, which the virtual work principle states, the IPAs' directions affect the dynamic behavior of spherical mechanisms. Thus, building a dynamic model that fully highlights their influence on the dynamic behavior is of interest during mechanism design to impose specific design requirements. For single-DOF spherical mechanisms, the

E-mail address: raffaele.digregorio@unife.it.

https://doi.org/10.1016/j.mechmachtheory.2025.106090
Received 28 March 2025; Received in revised form 21 May 2025; Accepted 22 May 2025
Available online 4 June 2025

Nomenclature

DOF	degree of freedom
SMC	spherical motion center
US	unit sphere
VC	velocity coefficient
VCV	velocity coefficient vector
ACJ	acceleration coefficient Jacobian
IPA_{ji}	instantaneous pole axis of the relative motion of link j with respect to link i in the multi-DOF spherical mechanism
$\mathbf{q}$	$(=(q_1, \ldots, q_n)^T)$ n-tuple collecting the n generalized coordinates, q_k for k=1, …, n, of an n-DOF spherical mechanism
${}^i\mathbf{v}_{P\|j}$	velocity of point P, fixed to link j, when observed (measured) from link i
${}^i\mathbf{a}_{P\|j}$	acceleration of point P, fixed to link j, when observed (measured) from link i
$\text{IPA}_{ji,k}$	instantaneous pole axis of the relative motion of link j with respect to link i in the single-DOF spherical mechanism generated from a multi-DOF spherical mechanism by locking all the generalized coordinates but the k-th, named q_k
$\mathbf{u}_{ji}$	unit vector parallel to IPA_{ji}
P_{ji}	intersection point of IPA_{ji} with the US which the unit vector $\mathbf{u}_{ji}$ points toward (Fig. 1)
$\mathbf{u}_{ji,k}$	unit vector parallel to $\text{IPA}_{ji,k}$
$\text{P}_{ji,k}$	intersection point of $\text{IPA}_{ji,k}$ with the US which the unit vector $\mathbf{u}_{ji,k}$ points toward
$\boldsymbol{\nu}_{\zeta/\mathbf{q}}$	$\left(=\nabla_{\mathbf{q}}(\zeta)=\left(\frac{\partial\zeta}{\partial q_1},\cdots,\frac{\partial\zeta}{\partial q_n}\right)^T=\left(\nu_{\zeta/\mathbf{q},1},\cdots,\nu_{\zeta/\mathbf{q},n}\right)^T\right)$ n-dimensional vector denoting the VCV with respect to $\mathbf{q}$ of the motion variable $\zeta=\zeta(q_1,\ldots,q_n)$
$\boldsymbol{\Lambda}_{\zeta/\mathbf{q}}$	$\left(=\mathbf{H}_{\mathbf{q}}(\zeta)=\left[\frac{\partial\boldsymbol{\nu}_{\zeta/\mathbf{q}}}{\partial q_1},\cdots,\frac{\partial\boldsymbol{\nu}_{\zeta/\mathbf{q}}}{\partial q_n}\right]=\left[\lambda_{\zeta/\mathbf{q},ji}\right]\right)$ the $n\times n$ symmetric matrix denoting the ACJ with respect to $\mathbf{q}$ of the motion variable $\zeta=\zeta(q_1,\ldots,q_n)$
$\omega_{ji}\mathbf{u}_{ji}$	$(=\boldsymbol{\omega}_{ji})$ angular velocity of the relative motion of link j with respect to link i in the multi-DOF spherical mechanism; ω_{ji} is its signed magnitude
$\omega_{ji,k}\mathbf{u}_{ji,k}$	$(=\boldsymbol{\omega}_{ji,k})$ angular velocity of the relative motion of link j with respect to link i in the single-DOF spherical mechanism generated from the multi-DOF spherical mechanism by locking all the generalized coordinates but the k-th, named q_k; $\omega_{ji,k}$ is its signed magnitude
$\nu_{ji,k}$	$\left(\nu_{ji,k}=\frac{\omega_{ji,k}}{\dot{q}_k}\right)$ VC of the k-th single-DOF mechanism (i.e., the single-DOF spherical mechanism generated from the multi-DOF spherical mechanism by locking all the generalized coordinates but the k-th, named q_k);
$\mathbf{U}_{ji}$	$\left(=\left[\nu_{ji,1}\mathbf{u}_{ji,1}\quad\cdots\quad\nu_{ji,n}\mathbf{u}_{ji,n}\right]\right)$ $3\times n$ matrix involved in Eq. (16) to write $\boldsymbol{\omega}_{ji}=\mathbf{U}_{ji}\dot{\mathbf{q}}$
$Ox_jy_jz_j$	Cartesian reference, fixed to link j, that has the origin, O, coincident with the SMC and the y_jz_j-coordinate plane coincident with the plane that contains the great circle that locates the pose of link j on the US (see Fig. 1)
${}^i\mathbf{R}_j$	rotation matrix that transforms vector components measured in $Ox_jy_jz_j$ into vector components measured in $Ox_iy_iz_i$
α_j	central angle subtended by the great circle arc of US that is fixed to link j
$(\cdot)\Big\|_{\left(\frac{\forall i\neq k}{\dot{q}_i=0}\right)}$	kinematic quantity $(\cdot)$ computed in the case in which all the generalized coordinates are locked but the k-th one (which coincides with the $(\cdot)$ computed in the single-DOF mechanism generated from the multi-DOF one by locking all the generalized coordinates but q_k)
$(\cdot)_{x,v}$	virtual value of the instantaneous kinematics' quantity $(\cdot)_x$, that is, value of $(\cdot)_x$ computed by considering the mechanism frame "frozen" at a given time instant
m_j	mass of link j
G_j	barycenter of link j
${}^jG_j$	position vector of the barycenter of link j measured in $Ox_jy_jz_j$
$\mathbf{I}_{O,j}$	inertia tensor of link j about point O
${}^j\mathbf{I}_{O,j}$	inertia tensor of link j about point O measured in $Ox_jy_jz_j$
$I_{(O,\mathbf{u}_{jf})}$	$\left(=\mathbf{u}_{jf}\cdot\left(\mathbf{I}_{O,j}\mathbf{u}_{jf}\right)\right)$ inertia moment of link j with respect to the line IPA_{jf}, which, in the front subscript, is indicated by giving, in the form $(O,\mathbf{u}_{jf})$, a point (i.e., O) of the line IPA_{jf} and a unit vector (i.e., $\mathbf{u}_{jf}$) parallel to IPA_{jf}
$\mathbf{F}_j$	resultant force of the system of forces applied to link j
$\mathbf{M}_{O,j}$	resultant moment about O of the system of forces applied to link j
$\mathbf{M}^e_{O,j}$	resultant moment about O of all the loads applied to link j when computed without considering the reaction forces coming from the joints
Q_k	k-th generalized force with k=1, …, n, defined by Eq. (28a)
$Q_{k,e}$	contribution to the k-th generalized force Q_k due to the active loads (external loads) applied to the links and not coming from the joints as constraint reactions
τ_k	$(=Q_k-Q_{k,e})$ contribution to the k-th generalized force Q_k due to the active loads (internal loads) exchanged among the

	links inside the joints as active or passive constraint reactions
$\mathbf{Q}_e$	$(=(Q_{1,e}\cdots Q_{n,e})^T)$ n-tuple collecting all the $Q_{k,e}$ for k=1, …, n
$\boldsymbol{\tau}$	$(=(\tau_1\cdots\tau_n)^T)$ n-tuple collecting all the generalized torques τ_k for k=1, …, n
d_{0k}	scalar coefficient defined by Eq. (28d)
$\mathbf{d}_0$	$(=(d_{01}\cdots d_{0n})^T)$ n-tuple collecting all the scalar coefficients d_{0k} for k=1, …, n
$\mathbf{d}_{1k}$	n-tuple defined by Eq. (28c)
$\mathbf{b}_k$	$(=(b_{1k}\cdots b_{nk})^T)$ n-tuple whose entries, b_{sk} for $s=1, \ldots, n$, are defined by Eq. (29a)
$\mathbf{B}$	$n\times n$ matrix defined by Eq. (32a)
$\mathbf{C}_k$	$(=[c_{srk}])$ $n\times n$ matrix whose generic sr entry, c_{srk} with $s, r=1, \ldots, n$, is defined by Eq. (29b)
$\mathbf{C}$	$n\times n$ matrix defined by Eq. (32a)

author developed such a model in a previous paper [28] by exploiting Eksergian's equation, which is specific of single-DOF mechanisms. For multi-DOF spherical mechanisms, developing such a model requires a different approach and has not been presented yet. D'Alembert principle seems suitable to build such a model for multi-DOF spherical mechanisms. In particular, it comes from virtual work principle and the virtual displacements [29] appearing in it are those admitted when the constraints are "frozen" at a given instant of time (i.e., the ones admissible with stationary frame). Therefore, a dynamic model built through it can take into account even the case of mobile frame and, when applied to single-DOF mechanisms, it would extend the formulation presented in [28] that holds only for stationary frame.

Here, the peculiarities of spherical mechanisms, the previous results on the IPAs and D'Alembert's principle are exploited to build a novel dynamic model of multi-DOF spherical mechanisms that directly and in explicit form relates the IPAs' directions and the dynamic behavior of such mechanisms. The proposed model can take into account a possible frame motion and lends itself to satisfy dynamic requirements during mechanism design. Its effectiveness is also illustrated by applying it to one relevant case study.

The paper is organized as follows. Section 2 provides the necessary background concepts, define the adopted notations and deduces the model. Then, section 3 applies the proposed formulation to one case study and section 4 discusses the obtained results. Eventually, section 5 draws the conclusions.

2. Materials and Methods

Revolute (R) pairs and rolling (Cr) or slipping (Cs) contacts are the only kinematic pairs that are present in spherical mechanisms. These three kinematic pairs generate only holonomic and time-independent (scleronomic) constraints when only spherical motion is possible. Consequently, in spherical mechanisms, the constraint system is always holonomic and only a mobile frame can generate a possible time-dependent (rheonomic) constraint. However, even in the case of a mobile frame, the relative motions between couples of links is time-independent, that is, the constraints between links remain scleronomic.

In an n-DOF mechanical system with holonomic and time-independent constraints, any motion variable, say ζ, is expressible either explicitly (by solving the constraint equation system) or implicitly (by the constraint equation system) as a function of the n-tuple, say $\mathbf{q}=(q_1, \ldots, q_n)^T$, that collects the n independent motion variables chosen as *generalized coordinates* of the system, that is, the following relationship holds

$$\zeta = \zeta(q_1, \ldots, q_n) \tag{1}$$

which yields

$$\dot{\zeta} = \sum_{k=1,n} \frac{\partial \zeta}{\partial q_k}\dot{q}_k = \dot{\mathbf{q}}^T \boldsymbol{\nu}_{\zeta/\mathbf{q}} \tag{2a}$$

$$\ddot{\zeta} = \sum_{k=1,n} \frac{\partial \zeta}{\partial q_k}\ddot{q}_k + \sum_{\substack{k=1,n \\ r=1,n}} \frac{\partial^2 \zeta}{\partial q_k \partial q_r}\dot{q}_k\dot{q}_r = \ddot{\mathbf{q}}^T \boldsymbol{\nu}_{\zeta/\mathbf{q}} + \dot{\mathbf{q}}^T \boldsymbol{\Lambda}_{\zeta/\mathbf{q}}\, \dot{\mathbf{q}} \tag{2b}$$

where the n-dimensional vector $\boldsymbol{\nu}_{\zeta/\mathbf{q}}$ $(=(\nu_{\zeta/\mathbf{q},1}, \cdots, \nu_{\zeta/\mathbf{q},n})^T)$ and the $n\times n$ symmetric matrix $\boldsymbol{\Lambda}_{\zeta/\mathbf{q}}$ $(=[\lambda_{\zeta/\mathbf{q},ji}])$ are the *velocity-coefficient vector* (VCV) and the *acceleration-coefficient Jacobian* (ACJ) [30] with respect to $\mathbf{q}$ of the motion variable ζ, respectively, and are defined as follows ($\nabla_{\mathbf{q}}(\cdot)$ and $\mathbf{H}_{\mathbf{q}}(\cdot)$ denote the gradient and the Hessian with respect to $\mathbf{q}$ of the scalar function $(\cdot)$, respectively)

$$\boldsymbol{\nu}_{\zeta/\mathbf{q}} = \nabla_{\mathbf{q}}(\zeta) = \left(\frac{\partial \zeta}{\partial q_1}, \cdots, \frac{\partial \zeta}{\partial q_n}\right)^T \tag{3a}$$

$$\boldsymbol{\Lambda}_{\zeta/\mathbf{q}} = \mathbf{H}_{\mathbf{q}}(\zeta) = \left[\frac{\partial \boldsymbol{\nu}_{\zeta/\mathbf{q}}}{\partial q_1}, \cdots, \frac{\partial \boldsymbol{\nu}_{\zeta/\mathbf{q}}}{\partial q_n}\right] \tag{3b}$$

The vector $\boldsymbol{\nu}_{\zeta/\mathbf{q}}$ and the matrix $\boldsymbol{\Lambda}_{\zeta/\mathbf{q}}$ depend only on the mechanism configuration (i.e., on $\mathbf{q}$) and the k-th component $\nu_{\zeta/\mathbf{q},k}$ $\left(=\frac{\partial \zeta}{\partial q_k}\right)$

of $\boldsymbol{\nu}_{\zeta/\mathbf{q}}$ is equal to the ratio, hereafter denoted $\frac{\dot{\zeta}}{\dot{q}_k}\Big|_{\left(\frac{\forall i\neq k}{\dot{q}_i=0}\right)}$, between $\dot{\zeta}$ and $\dot{q}_k$ in the case in which all the generalized coordinates are locked but the k-th one (see Eq. (2a)). Such a ratio coincides with the *velocity coefficient* $(\dot{\zeta}/\dot{q}_k)$ [31] of the single-DOF mechanism generated from the multi-DOF one by locking all the generalized coordinates but q_k. Hereafter, for the sake of brevity, this single-DOF mechanism will be referred to as "*k-th single-DOF mechanism*" and a generic kinematic parameter $(\cdot)_{xy}$ of the multi-DOF mechanism will be denoted $(\cdot)_{xy,k}$ when evaluated in the k-th single-DOF mechanism.

In single-DOF spherical mechanisms, all the velocity coefficients uniquely depend on the mechanism configuration and are explicitly expressible as a function of the IPAs' directions [25,28,32] through simple formulas that will be recalled in the next sub-section. Therefore, the VCVs of multi-DOF spherical mechanisms are explicitly expressible as functions of the IPA directions of the single-DOF mechanisms generated from it.

Virtual displacements/velocities of spherical mechanisms with mobile frame can be computed through the above reported relationships. Indeed, in the case of holonomic and time-dependent (rheonomic) constraints any motion variable, say ζ_{ij}, is explicitly or implicitly expressible as follows (t is the time)

$$\zeta_{ij} = \zeta_{ij}(q_1, \ldots, q_n, t) \tag{4}$$

Consequently, since virtual displacements/velocities are, by definition [29], displacements/velocities computed by considering the constraints "frozen" at a given instant of time, the following relationships hold for the actual rate, $\dot{\zeta}_{ij}$, and the virtual rate, $\dot{\zeta}_{ij,v}$, of ζ_{ij}:

$$\left.\begin{aligned} \dot{\zeta}_{ij} &= \sum_{k=1,n}\frac{\partial\zeta_{ij}}{\partial q_k}\dot{q}_k + \frac{\partial\zeta_{ij}}{\partial t} \\ \dot{\zeta}_{ij,v} &= \dot{\zeta}_{ij} - \frac{\partial\zeta_{ij}}{\partial t} = \sum_{k=1,n}\frac{\partial\zeta_{ij}}{\partial q_k}\dot{q}_k \end{aligned}\right\} \Rightarrow \frac{\partial\zeta_{ij}}{\partial q_k} = \frac{\dot{\zeta}_{ij,v}}{\dot{q}_k}\Big|_{\left(\frac{\forall i\neq k}{\dot{q}_i=0}\right)} \tag{5}$$

Hereafter, $(\cdot)_{x,v}$ will denote the virtual value of the instantaneous kinematics' quantity $(\cdot)_x$, that is, the value of $(\cdot)_x$ computed by considering the mechanism frame "frozen" at a given time instant.

2.1. Background

With reference to the relative motion of link i with respect to link j (hereafter named "relative motion ij"), let IPA_{ij} ($\mathrm{IPA}_{ij,k}$), $\mathbf{u}_{ij}$ ($\mathbf{u}_{ij,k}$) and ω_{ij} ($\omega_{ij,k}$) denote respectively its IPA, a unit vector parallel to its IPA and the signed magnitude of its angular velocity $\boldsymbol{\omega}_{ij}$ ($\boldsymbol{\omega}_{ij,k}$), with positive sign so defined that $\boldsymbol{\omega}_{ij}=\omega_{ij}\mathbf{u}_{ij}$ ($\boldsymbol{\omega}_{ij,k}=\omega_{ij,k}\mathbf{u}_{ij,k}$), in the multi-DOF spherical mechanism (in the k-th single-DOF spherical mechanism). The relative motion theorems [33] make the following relationships hold for these kinematic quantities

$$\mathrm{IPA}_{ji} = \mathrm{IPA}_{ij};\ \mathbf{u}_{ji} = \mathbf{u}_{ij};\ \omega_{ji} = -\omega_{ij} \tag{6a}$$

$$\mathrm{IPA}_{ji,k} = \mathrm{IPA}_{ij,k};\ \mathbf{u}_{ji,k} = \mathbf{u}_{ij,k};\ \omega_{ji,k} = -\omega_{ij,k} \tag{6b}$$

Since Eqs. (6) are simple and direct to use, hereafter, when counting the relative motions between links the relative motions ij and ji will be considered two different representations of the same relative motion and will be counted only once.

In a system of three links, say links i, j and p, only the three relative motions ji, jp and pi, are possible and the relative motion theorems [33] relate their angular velocities (i.e., $\boldsymbol{\omega}_{ji}$, $\boldsymbol{\omega}_{jp}$, and $\boldsymbol{\omega}_{pi}$) through the relationship

$$\omega_{ji}\mathbf{u}_{ji} = \omega_{jp}\mathbf{u}_{jp} + \omega_{pi}\mathbf{u}_{pi} \tag{7}$$

Eq. (7), in the case of spherical motion, demonstrates the Aronhold-Kennedy (A-K) theorem [1], which states: "*If the three links i, j, and p perform an instantaneous spherical motion with the same SMC, then IPA_{ji}, IPA_{jp}, and IPA_{pi} must lie on the same plane passing through the SMC*". Indeed, Eq. (7) when dot multiplied by $\mathbf{u}_{jp}\times\mathbf{u}_{pi}$, immediately yields the analytic expression of this coplanarity, that is:

$$\mathbf{u}_{ji}\cdot\left(\mathbf{u}_{jp}\times\mathbf{u}_{pi}\right) = 0 \tag{8}$$

The A-K theorem is an operative tool for determining the unknown directions of IPAs [26]. Indeed, in a system of four links, say links i, j, p and r, if the directions of IPA_{jp}, IPA_{ip}, IPA_{jr}, and IPA_{ir} are known, the fact that IPA_{ji} must simultaneously lie on the plane which IPA_{jp} and IPA_{ip} lie on (i.e., the one passing through the SMC and perpendicular to $\mathbf{u}_{jp}\times\mathbf{u}_{pi}$) and on the plane which IPA_{jr} and IPA_{ir} lie on (i.e., the one passing through the SMC and perpendicular to $\mathbf{u}_{jr}\times\mathbf{u}_{ri}$) leads to the conclusion that IPA_{ji} must be the intersection line shared by these two planes and that its direction is computable with the following simple formula:

$$\mathbf{u}_{ji} = \frac{\left(\mathbf{u}_{jp}\times\mathbf{u}_{pi}\right)\times\left(\mathbf{u}_{jr}\times\mathbf{u}_{ri}\right)}{\|\left(\mathbf{u}_{jp}\times\mathbf{u}_{pi}\right)\times\left(\mathbf{u}_{jr}\times\mathbf{u}_{ri}\right)\|} \tag{9}$$

In single-DOF spherical mechanisms, since all the links can only perform instantaneous rotations, the velocity coefficients (VCs) are always reducible to ratios between signed magnitudes of angular velocities of two particular relative motions: one for the signed magnitude at the VC numerator and the other for the signed magnitude of the VC denominator. As a consequence, only two types of VCs are possible: (i) the VCs in which the two signed magnitudes of angular velocities appearing in them share a common index in their

front subscripts, which are referable to a system of three bodies, say links *i, j* and *p*, and (ii) the VCs in which the two signed magnitudes of angular velocities appearing in them do not share any index in their front subscripts, which are referable to a system of four bodies, say links *i, j, p* and *r*. With reference to the k-th single-DOF spherical mechanism, the general explicit expressions of the VC as a function of the IPAs' directions are deducible as follows in the two cases.

In case (i), there are only three relative motions (i.e., *ji, jp* and *pi*) among three bodies, but only two are independent. Indeed, they are related by Eq. (7), which, with the notations of the k-th single-DOF mechanism, becomes $\omega_{ji,k}\mathbf{u}_{ji,k} = \omega_{jp,k}\mathbf{u}_{jp,k} + \omega_{pi,k}\mathbf{u}_{pi,k}$. The dot product of Eq. (7) by $\mathbf{u}_{ji,k} \times (\mathbf{u}_{jp,k} \times \mathbf{u}_{pi,k})$ gives (remind that $\omega_{pi,k} = -\omega_{ip,k}$)

$$\omega_{jp,k}\{\mathbf{u}_{jp,k} \cdot [\mathbf{u}_{ji,k} \times (\mathbf{u}_{jp,k} \times \mathbf{u}_{pi,k})]\} = \omega_{ip,k}\{\mathbf{u}_{pi,k} \cdot [\mathbf{u}_{ji,k} \times (\mathbf{u}_{jp,k} \times \mathbf{u}_{pi,k})]\} \tag{10}$$

which immediately provides the following general expression of the three bodies' VC as a function of the IPAs' directions (here the shared index is *p*)

$$\frac{\omega_{jp,k}}{\omega_{ip,k}} = \frac{\mathbf{u}_{pi,k} \cdot [\mathbf{u}_{ji,k} \times (\mathbf{u}_{jp,k} \times \mathbf{u}_{pi,k})]}{\mathbf{u}_{jp,k} \cdot [\mathbf{u}_{ji,k} \times (\mathbf{u}_{jp,k} \times \mathbf{u}_{pi,k})]} \equiv \frac{(\mathbf{u}_{jp,k} \times \mathbf{u}_{pi,k}) \cdot (\mathbf{u}_{ji,k} \times \mathbf{u}_{pi,k})}{(\mathbf{u}_{jp,k} \times \mathbf{u}_{pi,k}) \cdot (\mathbf{u}_{ji,k} \times \mathbf{u}_{jp,k})} \tag{11}$$

In case (ii), only six relative motions are possible among four bodies (i.e., the relative motions *ji, jp, pi, ri, jr*, and *pr*), but only three of them are independent. Indeed, the relative motion theorems [33] relate them through the following three equations (remind that $\omega_{pi,k} = -\omega_{ip,k}$)

$$\omega_{ji,k}\mathbf{u}_{ji,k} = \omega_{jp,k}\mathbf{u}_{jp,k} + \omega_{pi,k}\mathbf{u}_{pi,k} \tag{12a}$$

$$\omega_{jr,k}\mathbf{u}_{jr,k} = \omega_{jp,k}\mathbf{u}_{jp,k} + \omega_{pr,k}\mathbf{u}_{pr,k} \tag{12b}$$

$$\omega_{ir,k}\mathbf{u}_{ir,k} = -\omega_{pi,k}\mathbf{u}_{pi,k} + \omega_{pr,k}\mathbf{u}_{pr,k} \tag{12c}$$

which, by summing Eqs. (12a) and (12c), yield

$$\omega_{ji,k}\mathbf{u}_{ji,k} + \omega_{ir,k}\mathbf{u}_{ir,k} = \omega_{jp,k}\mathbf{u}_{jp,k} + \omega_{pr,k}\mathbf{u}_{pr,k} \tag{13}$$

whose dot product by $(\mathbf{u}_{ir,k} \times \mathbf{u}_{jp,k})$ immediately provides the general expression of the four bodies' VC as a function of the IPAs' directions as follows:

$$\omega_{ji,k}\mathbf{u}_{ji,k} \cdot (\mathbf{u}_{ir,k} \times \mathbf{u}_{jp,k}) = \omega_{pr,k}\mathbf{u}_{pr,k} \cdot (\mathbf{u}_{ir,k} \times \mathbf{u}_{jp,k}) \Rightarrow \frac{\omega_{ji,k}}{\omega_{pr,k}} = \frac{\mathbf{u}_{pr,k} \cdot (\mathbf{u}_{ir,k} \times \mathbf{u}_{jp,k})}{\mathbf{u}_{ji,k} \cdot (\mathbf{u}_{ir,k} \times \mathbf{u}_{jp,k})} \tag{14}$$

Moreover, since in the *k*-th single-DOF mechanism, the input rate $\dot{q}_k$ is either indeed or expressible through the signed magnitude of the angular velocity of the input link, the velocity coefficient

$$\nu_{ji,k} = \frac{\omega_{ji,k}}{\dot{q}_k} \tag{15}$$

can always be written in explicit form as a function of the IPAs' directions by using either Eqs. (11) or (14) according to the particular indices appearing in the front subscripts of numerator and denominator of $\nu_{ji,k}$.

In *n*-DOF mechanisms, the linearity and homogeneity of the instantaneous kinematics relationships make the superposition principle hold. Such a principle leads to the following relationships [25]:

$$\left.\begin{aligned}\boldsymbol{\omega}_{ji} &= \sum_{k=1,n} \boldsymbol{\omega}_{ji,k}\\ \boldsymbol{\omega}_{ji,k} &= \omega_{ji,k}\mathbf{u}_{ji,k}\\ \omega_{ji,k} &= \nu_{ji,k}\dot{q}_k\end{aligned}\right\} \Rightarrow \left\{\begin{aligned}&\boldsymbol{\omega}_{ji} = \sum_{k=1,n} (\nu_{ji,k}\mathbf{u}_{ji,k})\dot{q}_k = \mathbf{U}_{ji}\dot{\mathbf{q}}\\ &\textit{with}\\ &\mathbf{U}_{ji} = \begin{bmatrix}\nu_{ji,1}\mathbf{u}_{ji,1} & \cdots & \nu_{ji,n}\mathbf{u}_{ji,n}\end{bmatrix}\end{aligned}\right. \Rightarrow \dot{\omega}_{ji} = \sum_{k=1,n} (\nu_{ji,k}\mathbf{u}_{ji,k})\ddot{q}_k + \sum_{\substack{k=1,n\\ r=1,n}} \dot{q}_k\dot{q}_r \frac{\partial(\nu_{ji,k}\mathbf{u}_{ji,k})}{\partial q_r} \tag{16}$$

Eq. (16) is exploitable to relate the IPAs directions of the *n*-DOF mechanism to those of the generated single-DOF mechanisms as follows [25]:

$$\left.\begin{aligned}&\boldsymbol{\omega}_{ji} = \sum_{k=1,n} (\nu_{ji,k}\mathbf{u}_{ji,k})\dot{q}_k\\ &\boldsymbol{\omega}_{ji} = \omega_{ji}\mathbf{u}_{ji} \Rightarrow \left\{\begin{aligned}\mathbf{u}_{ji} &= \frac{\boldsymbol{\omega}_{ji}}{\| \boldsymbol{\omega}_{ji} \|}\\ \omega_{ji} &= \| \boldsymbol{\omega}_{ji} \|\end{aligned}\right.\end{aligned}\right\} \Rightarrow \left\{\begin{aligned}\mathbf{u}_{ji} &= \frac{\sum_{k=1,n} (\nu_{ji,k}\mathbf{u}_{ji,k})\dot{q}_k}{\| \sum_{k=1,n} (\nu_{ji,k}\mathbf{u}_{ji,k})\dot{q}_k \|} = \mathbf{u}_{ji}(q_1, ..., q_n, \dot{q}_1, ..., \dot{q}_n)\\ \omega_{ji} &= \| \sum_{k=1,n} (\nu_{ji,k}\mathbf{u}_{ji,k})\dot{q}_k \| = \omega_{ji}(q_1, ..., q_n, \dot{q}_1, ..., \dot{q}_n)\end{aligned}\right. \tag{17}$$

The motion of a rigid body, say link *j*, constrained to perform only spherical motions with the same SMC can be studied by

projecting it from the SMC onto a sphere (unit sphere (US)) with unitary radius and center at the projection center. Indeed, this projection generates a rigid spherical lamina that slides on the US when the rigid body moves and there is a one-to-one correspondence between the pose of the lamina on the US and the pose (orientation) of the rigid body in the space [1,26].

The pose of a rigid lamina on a sphere is identifiable by locating the pose of a great circle arc fixed to that lamina [1,26]. Fig. 1shows a great circle arc of the US that is fixed to the rigid spherical lamina associated to a generic link, say link *j*. With reference to Fig. 1, the following notation are introduced:

- point *O* is the SMC;
- link *f* is the frame of the *n*-DOF mechanism and $Ox_fy_fz_f$ is a Cartesian reference fixed to the frame;
- $Ox_jy_jz_j$ is a Cartesian reference, fixed to link *j*, with origin at the SMC (point O) and y_jz_j-coordinate plane containing the great circle arc fixed to link *j* and the SMC;
- α_j is the central angle subtended by the great circle arc fixed to link *j*;
- P_{jf} is the intersection of IPA_{jf} and US which the unit vector $\mathbf{u}_{jf}$ points toward.

2.2. Deduction of the dynamic model

A general motion of the mechanism frame (link *f*) with respect to an observer (inertial reference), hereafter named link 0, is assignable through the characteristic vectors $\left({}^0\mathbf{v}_{O|f}, \boldsymbol{\omega}_{f0}\right)$ for the velocity field and $\left({}^0\mathbf{a}_{O|f}, \dot{\boldsymbol{\omega}}_{f0}\right)$ for the acceleration field where ${}^0\mathbf{v}_{O|f}$ (${}^0\mathbf{a}_{O|f}$) denotes the velocity (the acceleration) of point O, fixed to link *f*, when observed (measured) from link 0. From now on, ${}^i\mathbf{v}_{P|j}$ (${}^i\mathbf{a}_{P|j}$) will denote the velocity (the acceleration) of point P, fixed to link *j*, when observed (measured) from link *i*.

Let δt be any elementary variation of time, *t*, so defined that the product ${}^0\mathbf{v}_{O|f,v}\delta t$ ($\boldsymbol{\omega}_{j0,v}\delta t$) coincides with the virtual displacement (virtual rotation around $IPA_{j0,v}$=IPA_{jf}) of point O (of link *j*), that is, with the elementary displacement (rotation) occurring when the frame is considered at rest at a given time instant. For a spherical mechanism with *l* links and a movable frame, the adopted notations lead to the following expression of the D'Alembert's principle

$$\sum_{j=1,l}\mathbf{F}_j\cdot{}^0\mathbf{v}_{O|f,v}\delta t+\sum_{j=1,l}\mathbf{M}_{Oj}\cdot\boldsymbol{\omega}_{j0,v}\delta t-\sum_{j=1,l}\left[m_j\left(G_j-O\right)\times{}^0\mathbf{a}_{O|j}+\mathbf{I}_{Oj}\dot{\boldsymbol{\omega}}_{j0}+\boldsymbol{\omega}_{j0}\times\left(\mathbf{I}_{Oj}\boldsymbol{\omega}_{j0}\right)\right]\cdot\boldsymbol{\omega}_{j0,v}\delta t=0 \tag{18}$$

where m_j, G_j, and $\mathbf{I}_{O,j}$ are the mass, the barycenter and the inertia tensor about point O of link *j*, respectively; whereas, $\mathbf{F}_j$ and $\mathbf{M}_{O,j}$ are the resultant force, applied to link *j* at point O, and the resultant moment about O, respectively, which the system of forces applied to link j is reducible to.

The relative motion theorems [33] and the above-reported definition of the virtual quantities lead to the following relationships

$$\left.\begin{array}{l}\boldsymbol{\omega}_{j0}=\boldsymbol{\omega}_{jf}+\boldsymbol{\omega}_{f0}\\ \boldsymbol{\omega}_{j0,v}=\boldsymbol{\omega}_{jf}\end{array}\right\}\Rightarrow\boldsymbol{\omega}_{j0}=\boldsymbol{\omega}_{j0,v}+\boldsymbol{\omega}_{f0} \tag{19a}$$

$${}^0\mathbf{v}_{O|f,v}=0;{}^0\mathbf{v}_{O|f}={}^0\mathbf{v}_{O|j}\quad\forall j=1,\ldots,l;{}^0\mathbf{a}_{O|f}={}^0\mathbf{a}_{O|j}\quad\forall j=1,\ldots,l \tag{19b}$$

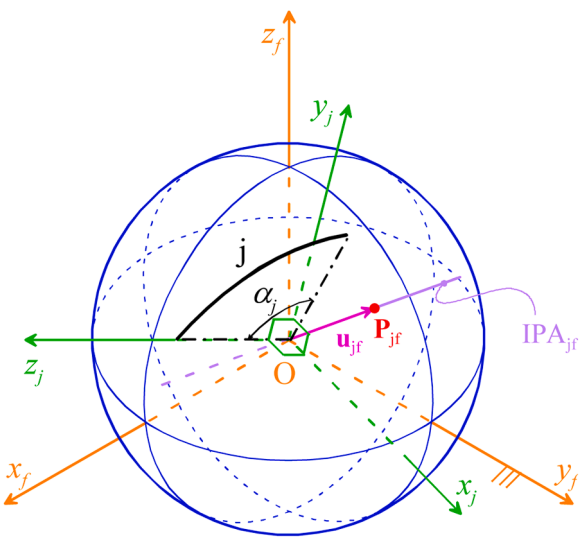

Fig. 1. A great circle arc of the US that is fixed to link *j* (reproduced from [28]): α_j is the central angle subtended by the arc, $Ox_jy_jz_j$ is a Cartesian reference, fixed to link *j*, with origin at the SMC (point O) and y_jz_j-coordinate plane containing the arc and the SMC, $Ox_fy_fz_f$ is a Cartesian reference fixed to mechanism's frame (link *f*).

$$\dot{\boldsymbol{\omega}}_{j0} = \dot{\boldsymbol{\omega}}_{jf} + \dot{\boldsymbol{\omega}}_{f0} + \boldsymbol{\omega}_{f0} \times \boldsymbol{\omega}_{jf} \tag{19c}$$

which allow the deduction of the following further formulas

$$\left.\begin{array}{c} \boldsymbol{\omega}_{j0} = \boldsymbol{\omega}_{j0,v} + \boldsymbol{\omega}_{f0} \\ \boldsymbol{\omega}_{j0,v} = \boldsymbol{\omega}_{jf} \\ \dot{\boldsymbol{\omega}}_{j0} = \dot{\boldsymbol{\omega}}_{jf} + \dot{\boldsymbol{\omega}}_{f0} + \boldsymbol{\omega}_{f0} \times \boldsymbol{\omega}_{jf} \\ \left[\boldsymbol{\omega}_{j0} \times \left(\mathbf{I}_{Oj}\boldsymbol{\omega}_{j0}\right) = \boldsymbol{\omega}_{j0,v} \times \left(\mathbf{I}_{Oj}\boldsymbol{\omega}_{j0,v}\right) + \boldsymbol{\omega}_{j0,v} \times \left(\mathbf{I}_{Oj}\boldsymbol{\omega}_{f0}\right) + \right. \\ \left. + \boldsymbol{\omega}_{f0} \times \left(\mathbf{I}_{Oj}\boldsymbol{\omega}_{j0,v}\right) + \boldsymbol{\omega}_{f0} \times \left(\mathbf{I}_{Oj}\boldsymbol{\omega}_{f0}\right) \right. \end{array}\right\} \Rightarrow \left[\begin{array}{c} \left[\boldsymbol{\omega}_{j0} \times \left(\mathbf{I}_{Oj}\boldsymbol{\omega}_{j0}\right)\right] \cdot \boldsymbol{\omega}_{j0,v} = \left[\boldsymbol{\omega}_{f0} \times \left(\mathbf{I}_{Oj}\boldsymbol{\omega}_{jf}\right) + \boldsymbol{\omega}_{f0} \times \left(\mathbf{I}_{Oj}\boldsymbol{\omega}_{f0}\right)\right] \cdot \boldsymbol{\omega}_{jf} \\ \left(\mathbf{I}_{Oj}\dot{\boldsymbol{\omega}}_{j0}\right) \cdot \boldsymbol{\omega}_{j0,v} = \left[\mathbf{I}_{Oj}\dot{\boldsymbol{\omega}}_{jf} + \mathbf{I}_{Oj}\dot{\boldsymbol{\omega}}_{f0} + \mathbf{I}_{Oj}\left(\boldsymbol{\omega}_{f0} \times \boldsymbol{\omega}_{jf}\right)\right] \cdot \boldsymbol{\omega}_{jf} \end{array}\right. \tag{20}$$

Moreover, the introduction of Eqs. (19) and (20) into Eq. (18) transforms it as follows:

$$\sum_{j=1,l}\left\{\mathbf{M}_{Oj} - \left[\mathbf{I}_{Oj}\dot{\boldsymbol{\omega}}_{jf} + \mathbf{I}_{Oj}\left(\boldsymbol{\omega}_{f0} \times \boldsymbol{\omega}_{jf}\right) + \boldsymbol{\omega}_{f0} \times \left(\mathbf{I}_{Oj}\boldsymbol{\omega}_{jf}\right) + m_j\left(G_j - O\right) \times {}^0\mathbf{a}_{Of} + \mathbf{I}_{Oj}\dot{\boldsymbol{\omega}}_{f0} + \boldsymbol{\omega}_{f0} \times \left(\mathbf{I}_{Oj}\boldsymbol{\omega}_{f0}\right)\right]\right\} \cdot \boldsymbol{\omega}_{jf}\delta t = 0 \tag{21}$$

which, by taking into account the relationship ($\widetilde{\mathbf{a}}$ denotes the skew-symmetric matrix associated to vector $\mathbf{a}$)

$$\left.\begin{array}{c} \mathbf{I}_{Oj}\left(\boldsymbol{\omega}_{f0} \times \boldsymbol{\omega}_{jf}\right) + \boldsymbol{\omega}_{f0} \times \left(\mathbf{I}_{Oj}\boldsymbol{\omega}_{jf}\right) = \left[\mathbf{I}_{Oj}\widetilde{\boldsymbol{\omega}}_{f0} + \widetilde{\boldsymbol{\omega}}_{f0}\mathbf{I}_{Oj}\right]\boldsymbol{\omega}_{jf} \\ \left[\mathbf{I}_{Oj}\widetilde{\boldsymbol{\omega}}_{f0}\right]^T = \left[\widetilde{\boldsymbol{\omega}}_{f0}\right]^T\mathbf{I}_{Oj} = -\widetilde{\boldsymbol{\omega}}_{f0}\mathbf{I}_{Oj} \\ \mathbf{I}_{Oj}\widetilde{\boldsymbol{\omega}}_{f0} = -\mathbf{I}_{Oj}\left(\widetilde{\boldsymbol{\omega}}_{f0}\right)^T = -\left[\widetilde{\boldsymbol{\omega}}_{f0}\mathbf{I}_{Oj}\right]^T \end{array}\right\} \Rightarrow \mathbf{I}_{Oj}\left(\boldsymbol{\omega}_{f0} \times \boldsymbol{\omega}_{jf}\right) + \boldsymbol{\omega}_{f0} \times \left(\mathbf{I}_{Oj}\boldsymbol{\omega}_{jf}\right) = \left\{\widetilde{\boldsymbol{\omega}}_{f0}\mathbf{I}_{Oj} - \left[\widetilde{\boldsymbol{\omega}}_{f0}\mathbf{I}_{Oj}\right]^T\right\}\boldsymbol{\omega}_{jf} \tag{22}$$

can be further simplified as follows

$$\sum_{j=1,l}\left\{\mathbf{M}_{Oj} - \left[\mathbf{I}_{Oj}\dot{\boldsymbol{\omega}}_{jf} + \left(\widetilde{\boldsymbol{\omega}}_{f0}\mathbf{I}_{Oj} - \left[\widetilde{\boldsymbol{\omega}}_{f0}\mathbf{I}_{Oj}\right]^T\right)\boldsymbol{\omega}_{jf} + m_j\left(G_j - O\right) \times {}^0\mathbf{a}_{Of} + \mathbf{I}_{Oj}\dot{\boldsymbol{\omega}}_{f0} + \boldsymbol{\omega}_{f0} \times \left(\mathbf{I}_{Oj}\boldsymbol{\omega}_{f0}\right)\right]\right\} \cdot \boldsymbol{\omega}_{jf}\delta t = 0 \tag{23}$$

The introduction of the $\boldsymbol{\omega}_{jf}$ expression coming from Eq. (16) (i.e., $\boldsymbol{\omega}_{jf} = \sum_{k=1,n}\left(\nu_{jf,k}\mathbf{u}_{jf,k}\right)\dot{q}_k$) into the elementary rotation $\boldsymbol{\omega}_{jf}\,\delta t$ transforms Eq. (23) as follows ($\delta q_k = \dot{q}_k\delta t$)

$$\sum_{k=1,n}\left\{\sum_{j=1,l}\nu_{jf,k}\left\{\mathbf{M}_{Oj} - \left[\mathbf{I}_{Oj}\dot{\boldsymbol{\omega}}_{jf} + \left(\widetilde{\boldsymbol{\omega}}_{f0}\mathbf{I}_{Oj} - \left[\widetilde{\boldsymbol{\omega}}_{f0}\mathbf{I}_{Oj}\right]^T\right)\boldsymbol{\omega}_{jf} + m_j\left(G_j - O\right) \times {}^0\mathbf{a}_{Of} + \mathbf{I}_{Oj}\dot{\boldsymbol{\omega}}_{f0} + \boldsymbol{\omega}_{f0} \times \left(\mathbf{I}_{Oj}\boldsymbol{\omega}_{f0}\right)\right]\right\} \cdot \mathbf{u}_{jf,k}\right\}\delta q_k = 0 \tag{24}$$

which, by considering that the virtual displacements δq_k for k=1, …, n are arbitrary and independent, leads to the following system of n scalar equations:

$$\sum_{j=1,l}\nu_{jf,k}\left(\mathbf{M}_{Oj} - \mathbf{I}_{Oj}\dot{\boldsymbol{\omega}}_{jf}\right) \cdot \mathbf{u}_{jf,k} = d_k; \quad k = 1,\ \cdots,\ n \tag{25}$$

where d_k has the following explicit expression

$$d_k = \sum_{j=1,l}\nu_{jf,k}\left[\left(\widetilde{\boldsymbol{\omega}}_{f0}\mathbf{I}_{Oj} - \left[\widetilde{\boldsymbol{\omega}}_{f0}\mathbf{I}_{Oj}\right]^T\right)\boldsymbol{\omega}_{jf} + m_j\left(G_j - O\right) \times {}^0\mathbf{a}_{Of} + \mathbf{I}_{Oj}\dot{\boldsymbol{\omega}}_{f0} + \boldsymbol{\omega}_{f0} \times \left(\mathbf{I}_{Oj}\boldsymbol{\omega}_{f0}\right)\right] \cdot \mathbf{u}_{jf,k}; \quad k = 1,\ \cdots,\ n \tag{26}$$

and collects all the terms depending on the frame motion. It is worth stressing that formula (26) makes all the scalar coefficients d_k vanish when the frame is at rest (i.e., when $\boldsymbol{\omega}_{f0}$, $\dot{\boldsymbol{\omega}}_{f0}$ and ${}^0\mathbf{a}_{Of}$ are all equal to zero).

If the expressions of $\boldsymbol{\omega}_{jf}$ and $\dot{\boldsymbol{\omega}}_{jf}$ coming from Eq. (16) are introduced into system (25), the following general dynamic model of an n-DOF spherical mechanism will be obtained

$$Q_k = \mathbf{b}_k^T\ddot{\mathbf{q}} + \dot{\mathbf{q}}^T\mathbf{C}_k\dot{\mathbf{q}} + \mathbf{d}_{1k}^T\dot{\mathbf{q}} + d_{0k}; \qquad k = 1,\ \cdots,\ n \tag{27}$$

with $d_k = \mathbf{d}_{1k}^T\dot{\mathbf{q}} + d_{0k}$ and

$$Q_k = \sum_{j=1,l}\nu_{jf,k}\mathbf{M}_{Oj} \cdot \mathbf{u}_{jf,k} = \tau_k + Q_{k,e} \ \Rightarrow\ Q_{k,e} = \sum_{j=1,l}\nu_{jf,k}\mathbf{M}_{Oj} \cdot \mathbf{u}_{jf,k} - \tau_k = \sum_{j=1,l}\nu_{jf,k}\mathbf{M}_{Oj}^e \cdot \mathbf{u}_{jf,k}; \qquad k = 1, \cdots, n \tag{28a}$$

$$\mathbf{b}_k = \begin{pmatrix} b_{1k} \\ \vdots \\ b_{nk} \end{pmatrix}; \mathbf{C}_k = \begin{bmatrix} c_{11k} & \cdots & c_{1nk} \\ \vdots & \ddots & \vdots \\ c_{n1k} & \cdots & c_{nnk} \end{bmatrix}; \qquad k = 1, \cdots, n \tag{28b}$$

$$\mathbf{d}_{1k}^T = \sum_{j=1,l} \nu_{jf,k} \mathbf{u}_{jf,k}^T \left(\widetilde{\boldsymbol{\omega}}_{f0} \mathbf{I}_{O,j} - \left[\widetilde{\boldsymbol{\omega}}_{f0} \mathbf{I}_{O,j} \right]^T \right) \mathbf{U}_{jf}; \qquad k = 1, \cdots, n \tag{28c}$$

$$d_{0k} = \sum_{j=1,l} \nu_{jf,k} \left[m_j (G_j - O) \times {}^0\mathbf{a}_{Of} + \mathbf{I}_{O,j} \dot{\boldsymbol{\omega}}_{f0} + \boldsymbol{\omega}_{f0} \times (\mathbf{I}_{O,j} \boldsymbol{\omega}_{f0}) \right] \cdot \mathbf{u}_{jf,k}; \qquad k = 1, \cdots, n \tag{28d}$$

where τ_k, hereafter named *k*-th *generalized torque*, is the contribution to Q_k due to the active forces coming from the joints (e.g., those generated from actuators and friction), $Q_{k,e}$ is the remaining part of Q_k (i.e., $Q_{k,e} = Q_k - \tau_k = \sum_{j=1,l} \nu_{jf,k} \mathbf{M}_{O,j}^e \cdot \mathbf{u}_{jf,k}$ where $\mathbf{M}_{O,j}^e$ is the resultant moment about *O* of all the loads applied to link *j* when computed without considering the reaction forces coming from the joints), and the following definitions have been introduced

$$b_{sk} = \sum_{j=1,l} \nu_{jf,s} \nu_{jf,k} \left(\mathbf{I}_{O,j} \mathbf{u}_{jf,s} \right) \cdot \mathbf{u}_{jf,k}; \qquad s = 1, \cdots, n \tag{29a}$$

$$c_{srk} = \sum_{j=1,l} \nu_{jf,k} \left[\mathbf{I}_{O,j} \frac{\partial \left(\nu_{jf,s} \mathbf{u}_{jf,s} \right)}{\partial q_r} \right] \cdot \mathbf{u}_{jf,k}; \qquad s, r = 1, \cdots, n \tag{29b}$$

It is worth noting that, since the inertia tensors $\mathbf{I}_{O,j}$ for *j*=1,…,*n* are all symmetric matrices, $\left(\mathbf{I}_{O,j} \mathbf{u}_{jf,s} \right) \cdot \mathbf{u}_{jf,k} = \left(\mathbf{I}_{O,j} \mathbf{u}_{jf,k} \right) \cdot \mathbf{u}_{jf,s}$, which makes Eq. (29a) lead to the following property: $b_{sk} = b_{ks}$.

System (27) is the sought-after general dynamic model which explicitly relates the IPAs' directions to the dynamic behavior of the *n*-DOF spherical mechanism. The constant parameters of this model are the geometric constants of links and joints plus the mass distribution data of the links. Moreover, regarding the variable parameters, $\mathbf{b}_k$ and $\mathbf{C}_k$ depend only on the mechanism configuration (i.e., on $\mathbf{q}$) through the IPAs' directions; whereas, $\mathbf{d}_{1k}$ and d_{0k} depend on the frame motion and on the mechanism configuration and they vanish when the frame is at rest.

2.3. Solution algorithms

Once the dynamic model of a mechanism has been built many types of problems can be addressed which refer to its design or its control or simply to its dynamic performance analysis. Nevertheless, only two of them are very often encountered in the majority of applications: (i) the direct dynamics' problem (DDP) and (ii) the inverse dynamics' problem (IDP). The DDP is the determination of the mechanism motion, that is, in our case, of $q_k(t)$ for *k*=1, …, *n*, when the initial motion conditions, that is, in our case, $q_k(0)$ and $\dot{q}_k(0)$ for *k*=1, …, *n*, together with the time histories of all the active loads, that is, of $Q_k(t)$ for *k*=1, …, *n*, are known. Vice Versa, the IDP is the determination of the time histories of the generalized torques, that is, in the case under study, of $\tau_k(t)$ for *k*=1, …, *n*, when the time histories of the generalized coordinates, that is, in our case, $q_k(t)$ for *k*=1, …, *n*, and of all the other active loads, that is, in our case, $Q_{k,e}(t)$ for *k*=1, …, *n*, are known.

Eq. (27) when used to solve the IDP generates a linear system of *n* algebraic equations, whose unknowns are $\tau_k(t)$ for *k*=1, …, *n*, which is immediately solvable in explicit form as follows

$$\tau_k = \mathbf{b}_k^T \ddot{\mathbf{q}} + \dot{\mathbf{q}}^T \mathbf{C}_k \dot{\mathbf{q}} + \mathbf{d}_{1k}^T \dot{\mathbf{q}} + d_{0k} - Q_{k,e}; \qquad k = 1, \cdots, n \tag{30}$$

The matrix form of system (30) is

$$\boldsymbol{\tau}(t) = \mathbf{B}(\mathbf{q}) \ddot{\mathbf{q}} + \mathbf{C}(\mathbf{q}, \dot{\mathbf{q}}, t) \dot{\mathbf{q}} + \mathbf{d}_0(\mathbf{q}, t) - \mathbf{Q}_e(\mathbf{q}, t) \tag{31}$$

where

$$\mathbf{B}(\mathbf{q}) = \begin{bmatrix} \mathbf{b}_1^T(\mathbf{q}) \\ \vdots \\ \mathbf{b}_n^T(\mathbf{q}) \end{bmatrix}; \mathbf{C}(\mathbf{q}, \dot{\mathbf{q}}, t) = \begin{bmatrix} \dot{\mathbf{q}}^T \mathbf{C}_1(\mathbf{q}) + \mathbf{d}_{11}^T(\mathbf{q}, t) \\ \vdots \\ \dot{\mathbf{q}}^T \mathbf{C}_n(\mathbf{q}) + \mathbf{d}_{1n}^T(\mathbf{q}, t) \end{bmatrix} \tag{32a}$$

$$\boldsymbol{\tau}(t) = \begin{pmatrix} \tau_1(t) \\ \vdots \\ \tau_n(t) \end{pmatrix}; \mathbf{d}_0(\mathbf{q}, t) = \begin{pmatrix} d_{01}(\mathbf{q}, t) \\ \vdots \\ d_{0n}(\mathbf{q}, t) \end{pmatrix}; \mathbf{Q}_e(\mathbf{q}, t) = \begin{pmatrix} Q_{1,e}(\mathbf{q}, t) \\ \vdots \\ Q_{n,e}(\mathbf{q}, t) \end{pmatrix} \tag{32b}$$

Conversely, when Eq. (27) is used to solve the DDP, it generates a non-linear system of *n* differential equations whose unknowns are the entries of the n-tuple $\mathbf{q}(t)$. This ODE system, in general, is solvable only by using numerical techniques.

Both the problems need the same preliminary kinematic analysis that starts from the constant parameters of the model (i.e., the

geometric constants and the mass distribution data), computes all the variable parameters depending on the mechanism configuration, that is, on $\mathbf{q}$, and build a database containing the computed values as a function of $\mathbf{q}$. These preliminary computations are implementable as follows (Fig. 2):

Preliminary Kinematic Analysis (PKA):

PKA.i) for k=1, …, n, the variation range of q_k is discretized, and a n-dimensional grid of $\mathbf{q}$ values is generated;
PKA.ii) for each $\mathbf{q}$ value of the grid generated in the previous step, the rotation matrices, ${}^f\mathbf{R}_j$ for $j\in\{1, \ldots, l \mid j\neq f\}$, that transform vector components measured in $Ox_jy_jz_j$ into vector components measured in $Ox_fy_fz_f$ are computed (i.e. the closure equations of the spherical mechanism are analytically or numerically solved);
PKA.iii) for k=1, …, n, by exploiting the rotation matrices, ${}^f\mathbf{R}_j$, determined in the previous step, the coordinates, measured in $Ox_fy_fz_f$, of the barycenters G_j for $j\in\{1, \ldots, l \mid j\neq f\}$ and the $\mathbf{u}_{jf,k}$ components, measured in $Ox_fy_fz_f$, of all the primary IPAs[1] of the k-th single-DOF spherical mechanism are immediately determined as functions of $\mathbf{q}$; successively, the $\mathbf{u}_{jf,k}$ components, measured in $Ox_fy_fz_f$, of its secondary IPAs are determined as functions of $\mathbf{q}$ by repeatedly using Eq. (9) in a suitable sequence (see [26] for details);
PKA.iv) by exploiting the $\mathbf{u}_{jf,k}$ unit vectors determined in the previous step, the necessary VCs, $\nu_{ji,k}$, as functions of $\mathbf{q}$ are determined by using the appropriate formula, that is, either Eq. (11) or Eq. (14);
PKA.v) by exploiting the VCs and the $\mathbf{u}_{jf,k}$ unit vectors as functions of $\mathbf{q}$, computed in the previous steps, and the mass distribution data of the links, the variable parameters, $\mathbf{b}_k$ and $\mathbf{C}_k$ as function of $\mathbf{q}$ are numerically/analytically computed through Eqs. (29a) and (29b).

The result of these preliminary computations is a database which, for each $\mathbf{q}$ value of the n-dimensional grid defined at step (PKA.i), gives ${}^f\mathbf{R}_j$[2], $\mathbf{u}_{jf}$, and G_j for $j\in\{1, \ldots, l \mid j\neq f\}$ together with $\mathbf{b}_k$ and $\mathbf{C}_k$ for k=1, …, n. This database is used to solve the specific dynamics' problem as explained below.

If the IDP must be solved, the data inputs are the time histories of the generalized coordinates, that is, $\mathbf{q}(t)$, of the frame motion, that is, ${}^0\mathbf{v}_{O|f}(t)$ and ${}^0\mathbf{R}_f(t)$, and of the active loads applied to the links, that is, all those involved in the computation of the $Q_{k,e}(t)$ for k=1, …, n by using formula (28a), together with the database generated from the PKA. Moreover, the output data are the time histories of the generalized torques applied by the actuators, that is, $\tau_k(t)$ for k=1, …, n. Such a computation can be implemented as follows (Fig. 3):

Inverse Dynamics' Problem (IDP) solution algorithm:

IDP.i) for a discretized set of time values, the data inputs $\mathbf{q}$(t), ${}^0\mathbf{v}_{O|f}(t)$ and ${}^0\mathbf{R}_f(t)$ are used to compute the corresponding values of $\dot{\mathbf{q}}(t)$, $\ddot{\mathbf{q}}(t)$, ${}^0\mathbf{a}_{O|f}(t)$, $\boldsymbol{\omega}_{f0}$(t) and $\dot{\boldsymbol{\omega}}_{f0}(t)$ (remind that $\widetilde{\boldsymbol{\omega}}_{f0} = {}^0\dot{\mathbf{R}}_f{}^0\mathbf{R}_f^T$ and $\dot{\widetilde{\boldsymbol{\omega}}}_{f0} = {}^0\ddot{\mathbf{R}}_f{}^0\mathbf{R}_f^T - \widetilde{\boldsymbol{\omega}}_{f0}\widetilde{\boldsymbol{\omega}}_{f0}$);
IDP.ii) for each value of $\mathbf{q}$(t) selected in the previous step by discretizing the time interval, the active loads applied to the links together with the $\nu_{jf,k}$ and $\mathbf{u}_{jf,k}$ data coming from the stored PKA database are used to compute the corresponding values of the $Q_{k,e}(t)$ for k=1, …, n by means of Eq. (28a);
IDP.iii) the results of step (IDP.i) together with the mass distribution data and the $\nu_{jf,k}$ and $\mathbf{u}_{jf,k}$ data coming from the stored PKA database are used to compute $d_{0k}(t)$ and $\mathbf{d}_{1k}(t)$ for k=1, …, n, by means of Eqs. (28c) and (28d);
IDP.iv) for each value of $\mathbf{q}$(t) selected at step (IDP.i), all the data computed in the previous steps together with the values of $\mathbf{b}_k$ and $\mathbf{C}_k$ for k=1, …, n, coming from the stored PKA database are used to compute the corresponding $\tau_k(t)$ for k=1, …, n, by means of Eq. (30).

If the DDP must be solved, the data inputs are the time histories of the generalized torques, that is, $\tau_k(t)$ for k=1, …, n, of the frame motion, that is, ${}^0\mathbf{v}_{O|f}(t)$ and ${}^0\mathbf{R}_f(t)$, and of the active loads applied to the links, that is, all those involved in the computation of the $Q_{k,e}(t)$ for k=1, …, n by using formula (28a), together with the database generated from the PKA and the initial condition of motion, that is, $\mathbf{q}$(0) and $\dot{\mathbf{q}}$(0). Moreover, the output data are the time histories of the generalized coordinates, that is, $\mathbf{q}(t)$. Such a computation can be implemented as follows (Fig. 4):

Direct Dynamics' Problem (DDP) solution algorithm:

DDP.i) for a discretized set of time values, the data inputs ${}^0\mathbf{v}_{O|f}(t)$ and ${}^0\mathbf{R}_f(t)$ are used to compute the corresponding values of ${}^0\mathbf{a}_{O|f}(t)$, $\boldsymbol{\omega}_{f0}$(t) and $\dot{\boldsymbol{\omega}}_{f0}(t)$ (remind that $\widetilde{\boldsymbol{\omega}}_{f0} = {}^0\dot{\mathbf{R}}_f{}^0\mathbf{R}_f^T$ and $\dot{\widetilde{\boldsymbol{\omega}}}_{f0} = {}^0\ddot{\mathbf{R}}_f{}^0\mathbf{R}_f^T - \widetilde{\boldsymbol{\omega}}_{f0}\widetilde{\boldsymbol{\omega}}_{f0}$);
DDP.ii) system (31) is rewritten as follows:

$$\ddot{\mathbf{q}}(t) = \mathbf{B}^{-1}(\mathbf{q})[\boldsymbol{\tau}(t) + \mathbf{Q}_e(\mathbf{q}, t) - \mathbf{C}(\mathbf{q}, \dot{\mathbf{q}}, t)\dot{\mathbf{q}}(t) - \mathbf{d}_0(\mathbf{q}, t)] \tag{33}$$

[1] Primary IPAs are those that can be located immediately, through a simple mechanism inspection, when the link poses are known; whereas secondary IPAs are those that are not primary. The positions of the secondary IPAs can be sequentially determined through known algorithms (see [26,27], for instance and further Refs.).
[2] It is worth noting that rotation matrices can be efficiently stored by using suitable orientation parameters (e.g., the Euler parameters [34])

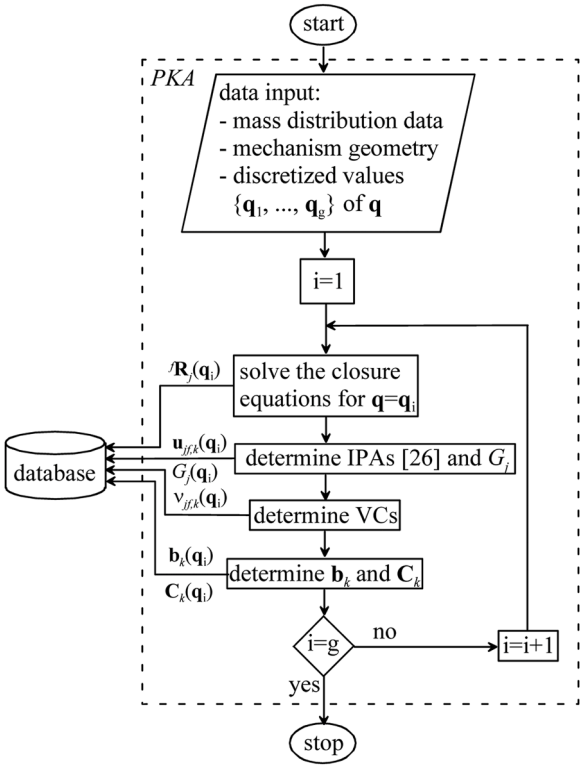

Fig. 2. Flow-chart of the PKA algorithm.

DDP.iii) the initial-motion data, $\mathbf{q}(0)$ and $\dot{\mathbf{q}}(0)$, and the other input data together with the results of step (DDP.i) and the data coming from the PKA database are used to start an iterative numerical algorithm that integrates system (33), which is a non-linear differential system of n equations in $\mathbf{q}(t)$, to compute $\mathbf{q}(t)$ by using an iterative formula of type

$$\mathbf{q}(t_{i+1}) = \mathbf{F}(\mathbf{q}(t_i), \mathbf{q}(t_{i-1}), t_{i+1}, t_i, t_{i-1}) \tag{34}$$

deduced from Eq. (33) (see [35] for details).

3. Results

In this section, the proposed formulation is applied to build the dynamic model of the spherical 5-bar linkage and to solve its IDP with three different set of active loads: (i) only inertia forces due to mechanism motion with frame at rest, (ii) inertia forces due to mechanism motion with frame at rest and external loads applied to the links, and (iii) inertia forces due to mechanism motion and to the motion of the frame.

The spherical 5-bar linkage (Fig. 5) is a 2-DOF single-looped linkage that enters in many applications (see [36–42], for instance). It consists of five binary links sequentially connected by R pairs whose axes share a common intersection point (point O in Fig. 5), which is the SMC.

Fig. 5 shows a generic spherical 5-bar linkage represented on the US with the notations of Fig. 1. With reference to Fig. 5, link 1 is the frame (i.e., f=1). The angles θ_{21} and θ_{51} are the two generalized coordinates q_1 and q_2, respectively, of the mechanism; whereas, the angle θ_{45} is the joint variable of the R pair connecting links 4 and 5. The two single-DOF mechanisms generated from the two-DOF mechanism of Fig. 5 are the two spherical 4-bar linkages shown in Fig. 6. In Figs. 5 and 6, the generic IPA$_{ji}$ (IPA$_{ji,k}$) direction, that is, $\mathbf{u}_{ji}$=P_{ji}−O ($\mathbf{u}_{ji,k}$=$P_{ji,k}$−O), is indicated by giving the point P_{ji} ($P_{ji,k}$) on the US. By using this convention, in Fig. 5, all the directions of the primary IPAs are indicated, that is, $\mathbf{u}_{21}$, $\mathbf{u}_{32}$, $\mathbf{u}_{43}$, $\mathbf{u}_{45}$, and $\mathbf{u}_{51}$. Moreover, in Fig. 6a (Fig. 6b), all the directions of the primary IPAs, that is, $\mathbf{u}_{21,1}$, $\mathbf{u}_{32,1}$, $\mathbf{u}_{43,1}$ and $\mathbf{u}_{41,1}$ ($\mathbf{u}_{31,2}$, $\mathbf{u}_{43,2}$, $\mathbf{u}_{45,2}$ and $\mathbf{u}_{51,2}$), are indicated together with the geometric determination of all the secondary IPAs, that is, $\mathbf{u}_{42,1}$ and $\mathbf{u}_{31,1}$ ($\mathbf{u}_{41,2}$ and $\mathbf{u}_{35,2}$).

3.1. PKA of the 5-bar linkage

From an analytic point of view, the following relationships hold (see Figs. 5 and 6):

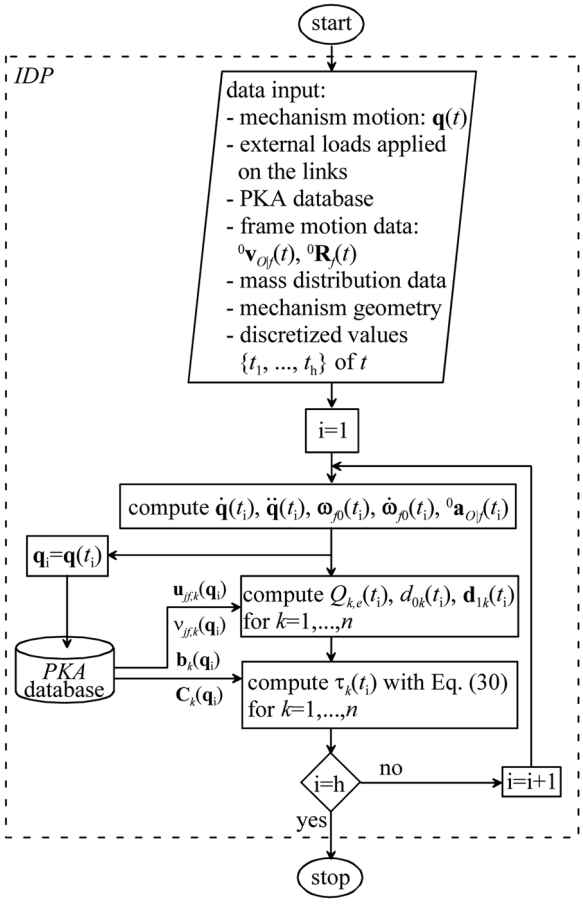

Fig. 3. Flow-chart of the IDP algorithm.

$$\mathbf{u}_{51} = \mathbf{u}_{51,2} = \mathbf{k}_1 = \mathbf{k}_5; \mathbf{k}_2 = \mathbf{u}_{21} = \mathbf{u}_{21,1} = \mathbf{k}_1 \cos\alpha_1 + \mathbf{j}_1 \sin\alpha_1 \tag{35a}$$

$$\mathbf{j}_2 = \mathbf{i}_1 \sin\theta_{21} + \cos\theta_{21}(\mathbf{k}_1 \sin\alpha_1 - \mathbf{j}_1 \cos\alpha_1); \mathbf{k}_3 = \mathbf{u}_{32} = \mathbf{u}_{32,1} = \mathbf{u}_{31,2} = \mathbf{k}_2 \cos\alpha_2 + \mathbf{j}_2 \sin\alpha_2 \tag{35b}$$

$$\mathbf{j}_5 = \mathbf{i}_1 \sin\theta_{51} - \mathbf{j}_1 \cos\theta_{51}; \mathbf{k}_4 = \mathbf{u}_{45} = \mathbf{u}_{45,2} = \mathbf{u}_{41,1} = \mathbf{k}_1 \cos\alpha_5 + \mathbf{j}_5 \sin\alpha_5 \tag{35c}$$

$$\mathbf{j}_4 = \frac{\mathbf{k}_1 \times \mathbf{k}_4}{\sin\alpha_5} \sin\theta_{45} + \cos\theta_{45}\left(\mathbf{j}_5 \cos\alpha_5 - \mathbf{k}_5 \sin\alpha_5\right); \mathbf{u}_{43} = \mathbf{u}_{43,2} = \mathbf{u}_{43,1} = \mathbf{k}_4 \cos\alpha_4 + \mathbf{j}_4 \sin\alpha_4 \tag{35d}$$

$$\mathbf{i}_3 = \frac{\mathbf{k}_3 \times \mathbf{u}_{43}}{\sin\alpha_3}; \mathbf{u}_{42,1} = \frac{(\mathbf{u}_{21} \times \mathbf{u}_{45}) \times (\mathbf{u}_{32} \times \mathbf{u}_{43})}{\| (\mathbf{u}_{21} \times \mathbf{u}_{45}) \times (\mathbf{u}_{32} \times \mathbf{u}_{43}) \|}; \mathbf{u}_{31,1} = \frac{(\mathbf{u}_{45} \times \mathbf{u}_{43}) \times (\mathbf{u}_{21} \times \mathbf{u}_{32})}{\| (\mathbf{u}_{45} \times \mathbf{u}_{43}) \times (\mathbf{u}_{21} \times \mathbf{u}_{32}) \|} \tag{35e}$$

$$\mathbf{u}_{35,2} = \frac{(\mathbf{u}_{45} \times \mathbf{u}_{43}) \times (\mathbf{u}_{51} \times \mathbf{u}_{32})}{\| (\mathbf{u}_{45} \times \mathbf{u}_{43}) \times (\mathbf{u}_{51} \times \mathbf{u}_{32}) \|}; \mathbf{u}_{41,2} = \frac{(\mathbf{u}_{32} \times \mathbf{u}_{43}) \times (\mathbf{u}_{51} \times \mathbf{u}_{45})}{\| (\mathbf{u}_{32} \times \mathbf{u}_{43}) \times (\mathbf{u}_{51} \times \mathbf{u}_{45}) \|} \tag{35f}$$

$$\mathbf{u}_{32} \cdot \mathbf{u}_{43} = \cos\alpha_3 \tag{35g}$$

$${}^f\mathbf{R}_j = \begin{bmatrix} \mathbf{i}_j & \mathbf{j}_j & \mathbf{k}_j \end{bmatrix}; \qquad j = 2, \cdots, 5 \tag{35h}$$

where $\mathbf{i}_j$, $\mathbf{j}_j$ and $\mathbf{k}_j$ for j=1,…,5 are the unit vectors of the coordinate axes x_j, y_j, and z_j, respectively, of the Cartesian reference $Ox_jy_jz_j$ fixed to link j (see Fig. 1); all the vector are measured in $Ox_fy_fz_f$. Moreover, let $G_j(\mathbf{q})$ and ${}^jG_j$ for j=2,…,5 be the position vectors of the barycenter G_j of link j measured in $Ox_fy_fz_f$ and in $Ox_jy_jz_j$, respectively, the explicit expression of $G_j(\mathbf{q})$ is given by the relationship $G_j(\mathbf{q})={}^f\mathbf{R}_j\,{}^jG_j$.

The introduction of the explicit expressions of $\mathbf{u}_{32}$ (Eq. (35b)) and $\mathbf{u}_{43}$ (Eq. (35d)) into Eq. (35g) yields the following closure equation:

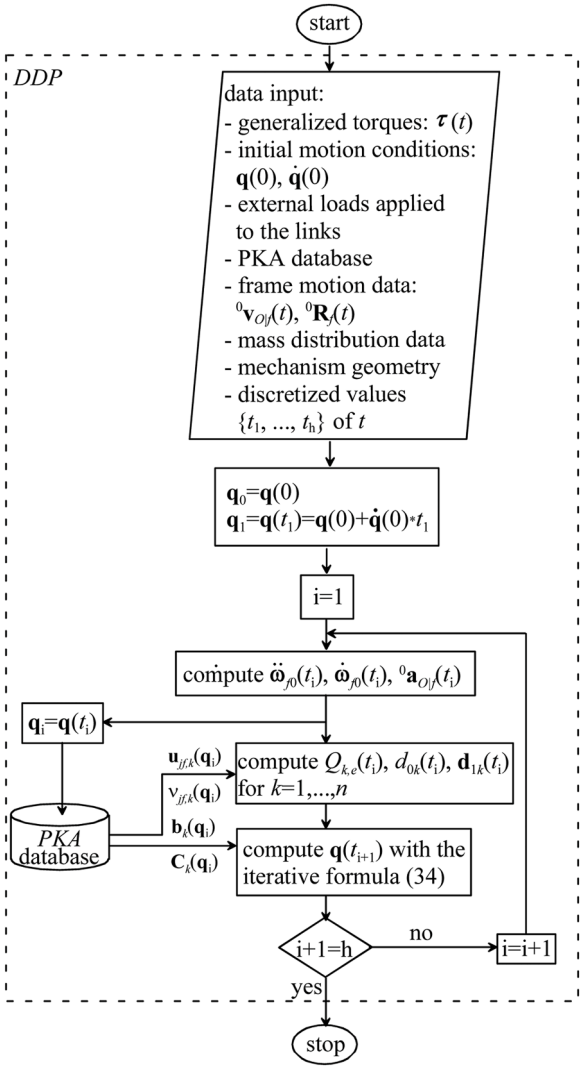

Fig. 4. Flow-chart of the DDP algorithm.

$$\begin{aligned}\cos\alpha_3 = {} & \sin\alpha_2\sin\theta_{21}[\cos\alpha_4\sin\alpha_5\sin\theta_{51} + \sin\alpha_4(\cos\theta_{51}\sin\theta_{45} + \cos\alpha_5\cos\theta_{45}\sin\theta_{51})]+\\ & +(\sin\alpha_1\cos\alpha_2 - \cos\alpha_1\sin\alpha_2\cos\theta_{21})[\sin\alpha_4(\sin\theta_{51}\sin\theta_{45} - \cos\alpha_5\cos\theta_{45}\cos\theta_{51}) - \cos\alpha_4\sin\alpha_5\cos\theta_{51}]+\\ & +(\cos\alpha_1\cos\alpha_2 + \sin\alpha_1\sin\alpha_2\cos\theta_{21})(\cos\alpha_4\cos\alpha_5 - \sin\alpha_4\sin\alpha_5\cos\theta_{45})\end{aligned} \tag{36}$$

which, after some algebraic manipulations, becomes

$$a_0 + a_1\sin\theta_{45} + a_2\cos\theta_{45} = 0 \tag{37}$$

where

$$\begin{aligned}a_0 &= \cos\alpha_4\{\sin\alpha_2[\sin\alpha_5\sin\theta_{21}\sin\theta_{51} + \cos\theta_{21}(\sin\alpha_1\cos\alpha_5 + \cos\alpha_1\sin\alpha_5\cos\theta_{51})] + \cos\alpha_2(\cos\alpha_1\cos\alpha_5 - \sin\alpha_1\sin\alpha_5\cos\theta_{51})\} - \cos\alpha_3\\ a_1 &= \sin\alpha_4[\sin\alpha_2\sin\theta_{21}\cos\theta_{51} + (\sin\alpha_1\cos\alpha_2 - \cos\alpha_1\sin\alpha_2\cos\theta_{21})\sin\theta_{51}]\\ a_2 &= \sin\alpha_4\{\cos\alpha_5[\sin\alpha_2\sin\theta_{21}\sin\theta_{51} - (\sin\alpha_1\cos\alpha_2 - \cos\alpha_1\sin\alpha_2\cos\theta_{21})\cos\theta_{51}] - (\cos\alpha_1\cos\alpha_2 + \sin\alpha_1\sin\alpha_2\cos\theta_{21})\sin\alpha_5\}\end{aligned} \tag{38}$$

Eq. (37) is solvable in closed form by transforming it into the quadratic equation $(a_0 - a_2)s^2 + 2sa_1 + (a_0 + a_2) = 0$, where s=tan$(\theta_{45}/2)$, through the half-tangent substitutions $\sin\theta_{45} = 2s/(1 + s^2)$ and $\cos\theta_{45} = (1-s^2)/(1 + s^2)$, and, then, solving the quadratic equation. This solution procedure yields the following closed form solutions

$$s_i = \frac{-a_1 + (-1)^i\sqrt{{a_1}^2 + {a_2}^2 - {a_0}^2}}{(a_0 - a_2)}; \qquad i = 1, 2 \tag{39}$$

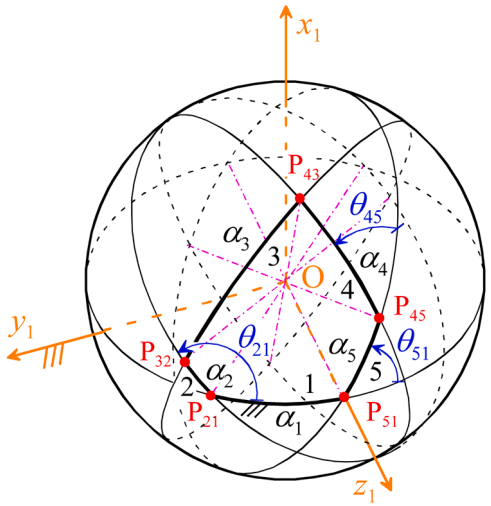

Fig. 5. Spherical 5-bar linkage represented on the US with the notations of Fig. 1.

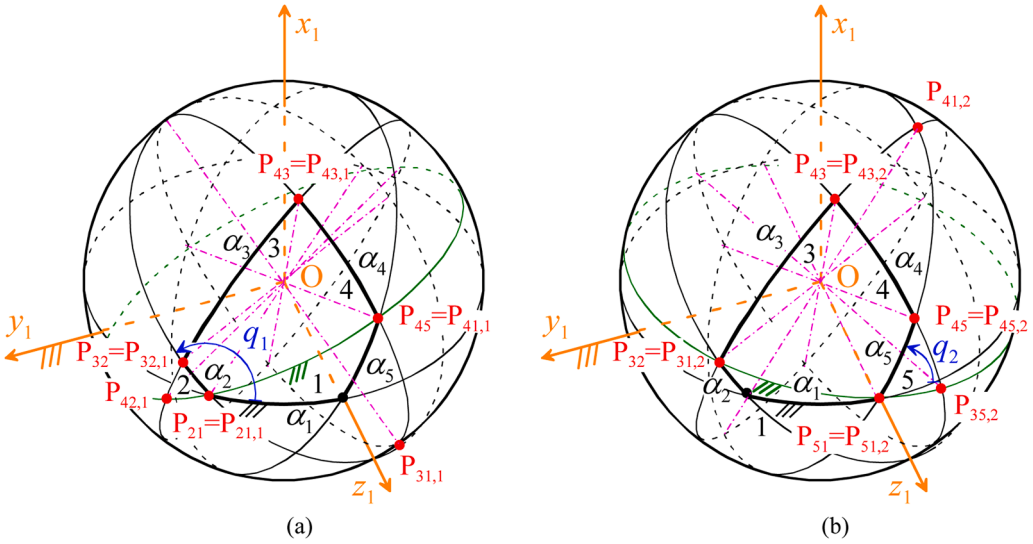

Fig. 6. Spherical 4-bar linkages generated from the spherical 5-bar linkage of Fig. 5 (the black circular dot denotes the locked R pair): (a) single-DOF linkage generated by locking q_2 ($=\theta_{51}$) and (b) single-DOF linkage generated by locking q_1 ($=\theta_{21}$).

Formula (39) gives the two values of θ_{45}, that is, $\theta_{45,i}$=2arctans$_i$ for $i = 1, 2$, corresponding to the two possible assembly modes that the spherical dyad constituted by links 3 ad 4 has for assigned values of the generalized coordinates θ_{21} and θ_{51}. The back substitution of the solving formula $\theta_{45,i}$=2arctans$_i$ into the formulas (35b)–(35f) and (35h) provides the explicit expressions of all the necessary IPA directions and rotation matrices as a function of the generalized coordinates (i.e., of the mechanism configuration). Fig. 7 shows the values of $\theta_{45,i}$ for $i = 1, 2$ as a function of the generalized coordinates θ_{21} and θ_{51} for the spherical 5-bar geometry reported in Table 1. It is worth stressing that all the discontinuities that appear in the diagrams of Fig. 7 correspond to jumps that are equal to multiples of 2π rad, that is, the angle values at the borders of the gap are equal to one another mod(2π) and, as a consequence, no physical jump occurs in θ_{45}.

Once the IPA directions have been determined, Eqs. (11) or (14) allow the determination of the explicit expressions of all the velocity coefficients $\nu_{jf,k}$, defined by Eq. (15) and with f=1, j=1,…,5 and k=1,2 that appear in the mechanism's dynamic model (Eq. (27) for this case study). In particular, the following relationships hold:

$$\nu_{11,1} = \nu_{51,1} = \nu_{11,2} = \nu_{21,2} = 0; \nu_{31,1} = \frac{\omega_{31,1}}{\dot{q}_1} = \frac{\omega_{31,1}}{\omega_{21,1}} = \frac{\omega_{31,1}}{\dot{\theta}_{21}} = \frac{(\mathbf{u}_{31,1} \times \mathbf{u}_{21}) \cdot (\mathbf{u}_{32} \times \mathbf{u}_{21})}{(\mathbf{u}_{31,1} \times \mathbf{u}_{21}) \cdot (\mathbf{u}_{32} \times \mathbf{u}_{31,1})} \tag{40a}$$

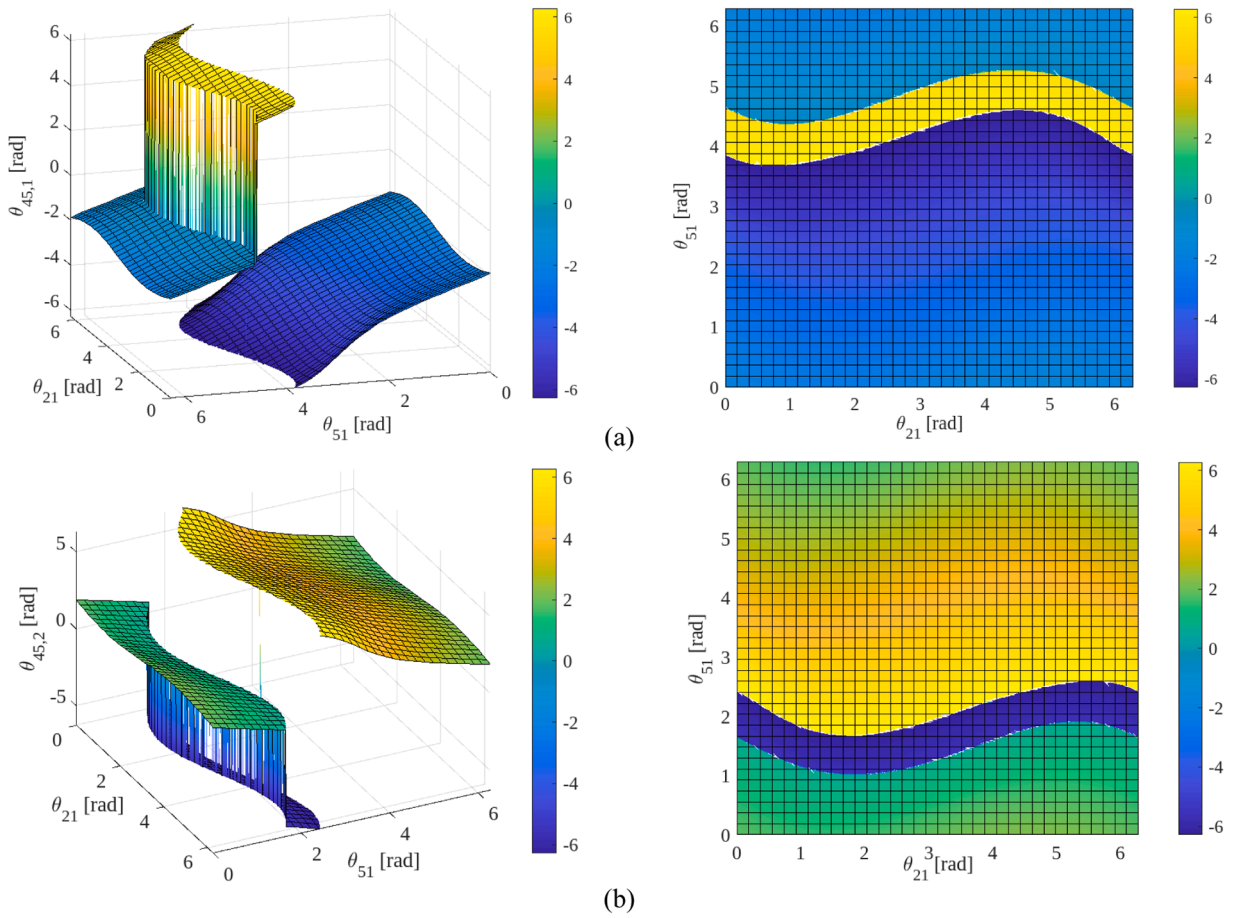

Fig. 7. Position analysis solution of the spherical 5-bar linkage with the geometry of Table 1: a) 3D view (left) and top view (right) of the diagram of $\theta_{45,1}$ (see Fig. 5 and Eq. (39)) as a function of the generalized coordinates θ_{21} and θ_{51}, and b) 3D view (left) and top view (right) of the diagram of $\theta_{45,2}$ (see Fig. 5 and Eq. (39)) as a function of the generalized coordinates θ_{21} and θ_{51}.

Table 1
Geometric and mass distribution data of the links of the spherical five-bar linkage used in the numerical example (^jG_j and $^j\mathrm{I}_{O,j}$ denote G_j and $\mathrm{I}_{O,j}$, respectively, when measured in $Ox_jy_jz_j$ (see Fig. 1)).

j	α_j [rad]	m_j [kg]	^jG_j [m]	$^j\mathrm{I}_{O,j}$ [kg m^2]
1	$\pi/3$	–	–	–
2	$\pi/9$	0.5	$\begin{pmatrix} 0 \\ 0.345536 \\ 1.959631 \end{pmatrix}$	$\begin{bmatrix} 2 & 0 & 0 \\ 0 & 1.920725 & -0.335117 \\ 0 & -0.335117 & 0.079275 \end{bmatrix}$
3	$7\pi/18$	1.75	$\begin{pmatrix} 0 \\ 1.077128 \\ 1.538298 \end{pmatrix}$	$\begin{bmatrix} 7 & 0 & 0 \\ 0 & 4.420725 & -2.529672 \\ 0 & -2.529672 & 2.579275 \end{bmatrix}$
4	$4\pi/9$	2	$\begin{pmatrix} 0 \\ 1.183662 \\ 1.410633 \end{pmatrix}$	$\begin{bmatrix} 8 & 0 & 0 \\ 0 & 4.489908 & -2.778405 \\ 0 & -2.778405 & 3.510092 \end{bmatrix}$
5	$\pi/9$	0.5	$\begin{pmatrix} 0 \\ 0.345536 \\ 1.959631 \end{pmatrix}$	$\begin{bmatrix} 2 & 0 & 0 \\ 0 & 1.920725 & -0.335117 \\ 0 & -0.335117 & 0.079275 \end{bmatrix}$

$$\nu_{21,1} = \nu_{51,2} = 1; \nu_{41,1} = \frac{\omega_{41,1}}{\dot{q}_1} = \frac{\omega_{41,1}}{\omega_{21,1}} = \frac{\omega_{41,1}}{\dot{\theta}_{21}} = \frac{(\mathbf{u}_{45} \times \mathbf{u}_{21}) \cdot (\mathbf{u}_{42,1} \times \mathbf{u}_{21})}{(\mathbf{u}_{45} \times \mathbf{u}_{21}) \cdot (\mathbf{u}_{42,1} \times \mathbf{u}_{45})} \tag{40b}$$

$$\nu_{31,2} = \frac{\omega_{31,2}}{\dot{q}_2} = \frac{\omega_{31,2}}{\omega_{51,2}} = \frac{\omega_{31,2}}{\dot{\theta}_{51}} = \frac{(\mathbf{u}_{32} \times \mathbf{u}_{51}) \cdot (\mathbf{u}_{35,2} \times \mathbf{u}_{51})}{(\mathbf{u}_{32} \times \mathbf{u}_{51}) \cdot (\mathbf{u}_{35,2} \times \mathbf{u}_{32})} \tag{40c}$$

$$\nu_{41,2} = \frac{\omega_{41,2}}{\dot{q}_2} = \frac{\omega_{41,2}}{\omega_{51,2}} = \frac{\omega_{41,2}}{\dot{\theta}_{51}} = \frac{(\mathbf{u}_{41,2} \times \mathbf{u}_{51}) \cdot (\mathbf{u}_{45} \times \mathbf{u}_{51})}{(\mathbf{u}_{41,2} \times \mathbf{u}_{51}) \cdot (\mathbf{u}_{45} \times \mathbf{u}_{41,2})} \tag{40d}$$

Figs. 8, 9, 10 and 11 show the values of $\nu_{31,1}^{(i)}$, $\nu_{31,2}^{(i)}$, $\nu_{41,1}^{(i)}$ and $\nu_{41,2}^{(i)}$, respectively, where $i = 1, 2$ refers to the position analysis solution given by Eq. (39), as a function of the generalized coordinates θ_{21} and θ_{51} for the spherical 5-bar geometry reported in Table 1.

Eventually, by exploiting the deduced explicit expressions of the IPA directions and of the VCs, the explicit expressions of $\mathbf{b}_k$ and $\mathbf{C}_k$ for k=1,2 as a function of the generalized coordinates are immediately writable through Eqs. (29a) and (29b), respectively. In particular, the following relationships hold:

$$\mathbf{b}_1 = \begin{pmatrix} b_{11} \\ b_{21} \end{pmatrix}; \mathbf{b}_2 = \begin{pmatrix} b_{12} \\ b_{22} \end{pmatrix}; \mathbf{C}_1 = \begin{bmatrix} c_{111} & c_{121} \\ c_{211} & c_{221} \end{bmatrix}; \mathbf{C}_2 = \begin{bmatrix} c_{112} & c_{122} \\ c_{212} & c_{222} \end{bmatrix} \tag{41}$$

where

$$b_{11} = \sum_{j=1,5} \nu_{j1,1}\nu_{j1,1}(\mathbf{I}_{O,j}\mathbf{u}_{j1,1}) \cdot \mathbf{u}_{j1,1} = (\mathbf{I}_{O,2}\mathbf{u}_{21}) \cdot \mathbf{u}_{21} + \nu_{31,1}{}^2(\mathbf{I}_{O,3}\mathbf{u}_{31,1}) \cdot \mathbf{u}_{31,1} + \nu_{41,1}{}^2(\mathbf{I}_{O,4}\mathbf{u}_{45}) \cdot \mathbf{u}_{45} \tag{42a}$$

$$b_{12} = b_{21} = \sum_{j=1,5} \nu_{j1,2}\nu_{j1,1}(\mathbf{I}_{O,j}\mathbf{u}_{j1,2}) \cdot \mathbf{u}_{j1,1} = \nu_{31,2}\nu_{31,1}(\mathbf{I}_{O,3}\mathbf{u}_{32}) \cdot \mathbf{u}_{31,1} + \nu_{41,2}\nu_{41,1}(\mathbf{I}_{O,4}\mathbf{u}_{41,2}) \cdot \mathbf{u}_{45} \tag{42b}$$

$$b_{22} = \sum_{j=1,5} \nu_{j1,2}\nu_{j1,2}(\mathbf{I}_{O,j}\mathbf{u}_{j1,2}) \cdot \mathbf{u}_{j1,2} = (\mathbf{I}_{O,5}\mathbf{u}_{51}) \cdot \mathbf{u}_{51} + \nu_{41,2}{}^2(\mathbf{I}_{O,4}\mathbf{u}_{41,2}) \cdot \mathbf{u}_{41,2} + \nu_{31,2}{}^2(\mathbf{I}_{O,3}\mathbf{u}_{32}) \cdot \mathbf{u}_{32} \tag{42c}$$

$$c_{111} = \sum_{j=1,5} \nu_{j1,1}\left[\mathbf{I}_{O,j}\frac{\partial(\nu_{j1,1}\mathbf{u}_{j1,1})}{\partial\theta_{21}}\right] \cdot \mathbf{u}_{j1,1} = \nu_{31,1}\left[\mathbf{I}_{O,3}\frac{\partial(\nu_{31,1}\mathbf{u}_{31,1})}{\partial\theta_{21}}\right] \cdot \mathbf{u}_{31,1} + \nu_{41,1}\left[\mathbf{I}_{O,4}\frac{\partial(\nu_{41,1}\mathbf{u}_{45})}{\partial\theta_{21}}\right] \cdot \mathbf{u}_{45} \tag{42d}$$

$$c_{121} = \sum_{j=1,5} \nu_{j1,1}\left[\mathbf{I}_{O,j}\frac{\partial(\nu_{j1,1}\mathbf{u}_{j1,1})}{\partial\theta_{51}}\right] \cdot \mathbf{u}_{j1,1} = \nu_{31,1}\left[\mathbf{I}_{O,3}\frac{\partial(\nu_{31,1}\mathbf{u}_{31,1})}{\partial\theta_{51}}\right] \cdot \mathbf{u}_{31,1} + \nu_{41,1}\left[\mathbf{I}_{O,4}\frac{\partial(\nu_{41,1}\mathbf{u}_{45})}{\partial\theta_{51}}\right] \cdot \mathbf{u}_{45} \tag{42e}$$

$$c_{211} = \sum_{j=1,5} \nu_{j1,1}\left[\mathbf{I}_{O,j}\frac{\partial(\nu_{j1,2}\mathbf{u}_{j1,2})}{\partial\theta_{21}}\right] \cdot \mathbf{u}_{j1,1} = \nu_{31,1}\left[\mathbf{I}_{O,3}\frac{\partial(\nu_{31,2}\mathbf{u}_{32})}{\partial\theta_{21}}\right] \cdot \mathbf{u}_{31,1} + \nu_{41,1}\left[\mathbf{I}_{O,4}\frac{\partial(\nu_{41,2}\mathbf{u}_{41,2})}{\partial\theta_{21}}\right] \cdot \mathbf{u}_{45} \tag{42f}$$

$$c_{221} = \sum_{j=1,5} \nu_{j1,1}\left[\mathbf{I}_{O,j}\frac{\partial(\nu_{j1,2}\mathbf{u}_{j1,2})}{\partial\theta_{51}}\right] \cdot \mathbf{u}_{j1,1} = \nu_{31,1}\left[\mathbf{I}_{O,3}\frac{\partial(\nu_{31,2}\mathbf{u}_{32})}{\partial\theta_{51}}\right] \cdot \mathbf{u}_{31,1} + \nu_{41,1}\left[\mathbf{I}_{O,4}\frac{\partial(\nu_{41,2}\mathbf{u}_{41,2})}{\partial\theta_{51}}\right] \cdot \mathbf{u}_{45} \tag{42g}$$

$$c_{112} = \sum_{j=1,5} \nu_{j1,2}\left[\mathbf{I}_{O,j}\frac{\partial(\nu_{j1,1}\mathbf{u}_{j1,1})}{\partial\theta_{21}}\right] \cdot \mathbf{u}_{j1,2} = \nu_{31,2}\left[\mathbf{I}_{O,3}\frac{\partial(\nu_{31,1}\mathbf{u}_{31,1})}{\partial\theta_{21}}\right] \cdot \mathbf{u}_{32} + \nu_{41,2}\left[\mathbf{I}_{O,4}\frac{\partial(\nu_{41,1}\mathbf{u}_{45})}{\partial\theta_{21}}\right] \cdot \mathbf{u}_{41,2} \tag{42h}$$

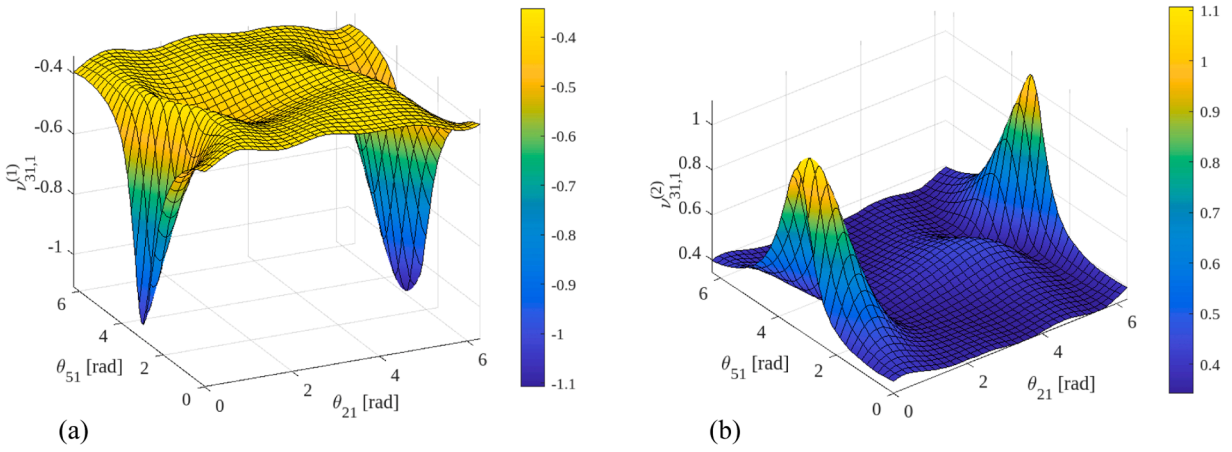

Fig. 8. Diagrams of $\nu_{31,1}^{(i)}$ for $i = 1$ (a) and $i = 2$ (b), where $i = 1, 2$ refers to the position analysis solution given by Eq. (39), as a function of the generalized coordinates θ_{21} and θ_{51} for the spherical 5-bar geometry reported in Table 1.

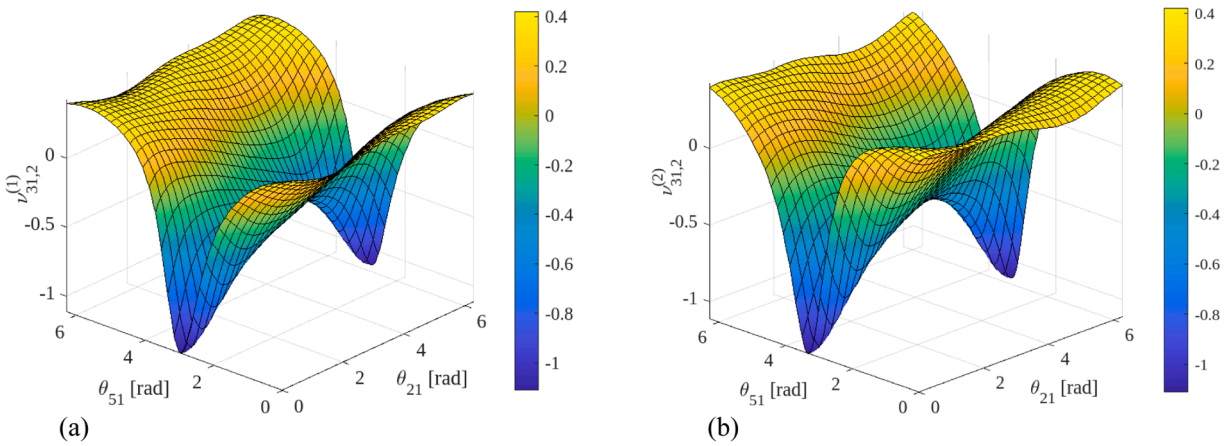

Fig. 9. Diagrams of $\nu^{(i)}_{31,2}$ for $i = 1$ (a) and $i = 2$ (b), where $i = 1, 2$ refers to the position analysis solution given by Eq. (39), as a function of the generalized coordinates θ_{21} and θ_{51} for the spherical 5-bar geometry reported in Table 1.

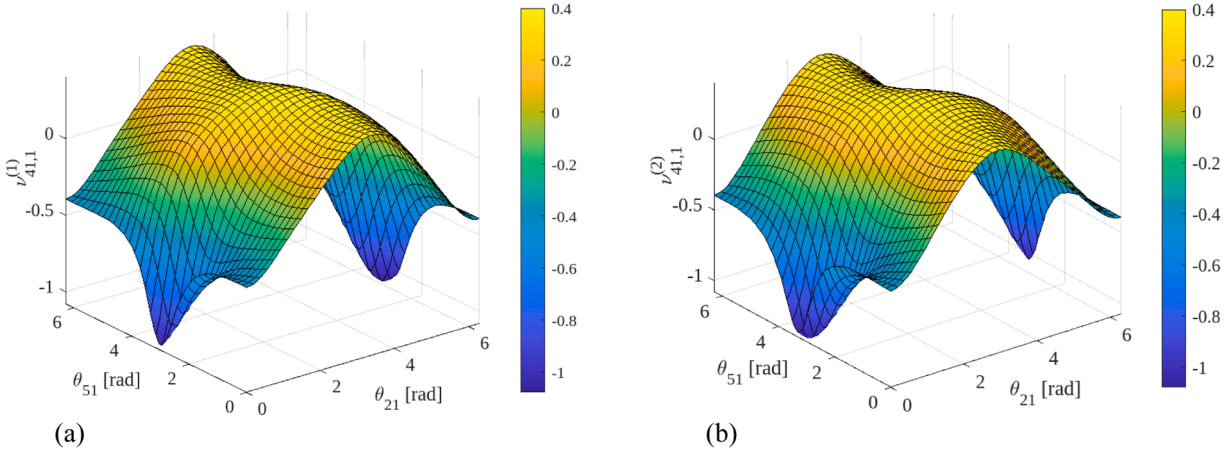

Fig. 10. Diagrams of $\nu^{(i)}_{41,1}$ for $i = 1$ (a) and $i = 2$ (b), where $i = 1, 2$ refers to the position analysis solution given by Eq. (39), as a function of the generalized coordinates θ_{21} and θ_{51} for the spherical 5-bar geometry reported in Table 1.

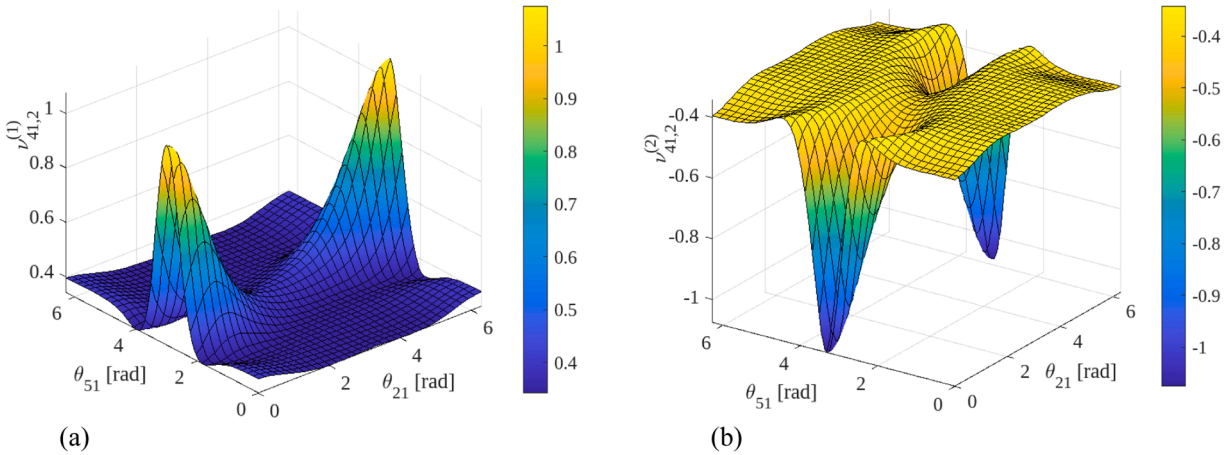

Fig. 11. Diagrams of $\nu^{(i)}_{41,2}$ for $i = 1$ (a) and $i = 2$ (b), where $i = 1, 2$ refers to the position analysis solution given by Eq. (39), as a function of the generalized coordinates θ_{21} and θ_{51} for the spherical 5-bar geometry reported in Table 1.

$$c_{122}=\sum_{j=1,5}\nu_{j1,2}\left[\mathbf{I}_{O,j}\frac{\partial\left(\nu_{j1,1}\mathbf{u}_{j1,1}\right)}{\partial\theta_{51}}\right]\cdot\mathbf{u}_{j1,2}=\nu_{31,2}\left[\mathbf{I}_{O,3}\frac{\partial\left(\nu_{31,1}\mathbf{u}_{31,1}\right)}{\partial\theta_{51}}\right]\cdot\mathbf{u}_{32}+\nu_{41,2}\left[\mathbf{I}_{O,4}\frac{\partial\left(\nu_{41,1}\mathbf{u}_{45}\right)}{\partial\theta_{51}}\right]\cdot\mathbf{u}_{41,2} \tag{42i}$$

$$c_{212}=\sum_{j=1,5}\nu_{j1,2}\left[\mathbf{I}_{O,j}\frac{\partial\left(\nu_{j1,2}\mathbf{u}_{j1,2}\right)}{\partial\theta_{21}}\right]\cdot\mathbf{u}_{j1,2}=\nu_{31,2}\left[\mathbf{I}_{O,3}\frac{\partial\left(\nu_{31,2}\mathbf{u}_{32}\right)}{\partial\theta_{21}}\right]\cdot\mathbf{u}_{32}+\nu_{41,2}\left[\mathbf{I}_{O,4}\frac{\partial\left(\nu_{41,2}\mathbf{u}_{41,2}\right)}{\partial\theta_{21}}\right]\cdot\mathbf{u}_{41,2} \tag{42j}$$

$$c_{222}=\sum_{j=1,5}\nu_{j1,2}\left[\mathbf{I}_{O,j}\frac{\partial\left(\nu_{j1,2}\mathbf{u}_{j1,2}\right)}{\partial\theta_{51}}\right]\cdot\mathbf{u}_{j1,2}=\nu_{31,2}\left[\mathbf{I}_{O,3}\frac{\partial\left(\nu_{31,2}\mathbf{u}_{32}\right)}{\partial\theta_{51}}\right]\cdot\mathbf{u}_{32}+\nu_{41,2}\left[\mathbf{I}_{O,4}\frac{\partial\left(\nu_{41,2}\mathbf{u}_{41,2}\right)}{\partial\theta_{51}}\right]\cdot\mathbf{u}_{41,2} \tag{42k}$$

When explicit formulas are available, they replace the PKA database during the solution of the dynamics' problems. Therefore, all the above-deduced explicit formulas will play the role of the PKA database in the following part of this section.

3.2. IDP solution of the 5-bar linkage

The introduction of the above-deduced formulas into Eq. (30) provides the following dynamic model of the spherical 5-bar linkage

$$\begin{pmatrix}\tau_1\\ \tau_2\end{pmatrix}=\begin{bmatrix}\mathbf{b}_1^T\\ \mathbf{b}_2^T\end{bmatrix}\begin{pmatrix}\ddot{\theta}_{21}\\ \ddot{\theta}_{51}\end{pmatrix}+\begin{bmatrix}(\dot{\theta}_{21}\quad\dot{\theta}_{51})\mathbf{C}_1+\mathbf{d}_{11}^T\\ (\dot{\theta}_{21}\quad\dot{\theta}_{51})\mathbf{C}_2+\mathbf{d}_{12}^T\end{bmatrix}\begin{pmatrix}\dot{\theta}_{21}\\ \dot{\theta}_{51}\end{pmatrix}+\begin{pmatrix}d_{01}\\ d_{02}\end{pmatrix}-\begin{pmatrix}Q_{1,e}\\ Q_{2,e}\end{pmatrix} \tag{43}$$

where

$$Q_{1,e}=\sum_{j=1,5}\nu_{j1,1}\mathbf{M}_{O,j}^e\cdot\mathbf{u}_{j1,1}=\mathbf{M}_{O,2}^e\cdot\mathbf{u}_{21}+\nu_{31,1}\mathbf{M}_{O,3}^e\cdot\mathbf{u}_{31,1}+\nu_{41,1}\mathbf{M}_{O,4}^e\cdot\mathbf{u}_{45} \tag{44a}$$

$$Q_{2,e}=\sum_{j=1,5}\nu_{j1,2}\mathbf{M}_{O,j}^e\cdot\mathbf{u}_{j1,2}=\nu_{31,2}\mathbf{M}_{O,3}^e\cdot\mathbf{u}_{32}+\nu_{41,2}\mathbf{M}_{O,4}^e\cdot\mathbf{u}_{41,2}+\mathbf{M}_{O,5}^e\cdot\mathbf{u}_{51} \tag{44b}$$

$$\left.\begin{array}{l}\mathbf{d}_{1k}^T=\sum_{j=2,5}\nu_{j1,k}\mathbf{u}_{j1,k}^T\left(\widetilde{\boldsymbol{\omega}}_{10}\mathbf{I}_{Oj}-\left[\widetilde{\boldsymbol{\omega}}_{10}\mathbf{I}_{Oj}\right]^T\right)\left[\nu_{j1,1}\mathbf{u}_{j1,1}\quad\nu_{j1,2}\mathbf{u}_{j1,2}\right]\\ \text{with } k=1,2\end{array}\right\}\Rightarrow$$

$$\left\{\begin{array}{l}\left[\begin{array}{l}\mathbf{d}_{11}^T=\mathbf{u}_{21}^T\left(\widetilde{\boldsymbol{\omega}}_{10}\mathbf{I}_{O,2}-\left[\widetilde{\boldsymbol{\omega}}_{10}\mathbf{I}_{O,2}\right]^T\right)\left[\mathbf{u}_{21}\ \mathbf{0}\right]+\\ +\nu_{31,1}\mathbf{u}_{31,1}^T\left(\widetilde{\boldsymbol{\omega}}_{10}\mathbf{I}_{O,3}-\left[\widetilde{\boldsymbol{\omega}}_{10}\mathbf{I}_{O,3}\right]^T\right)\left[\nu_{31,1}\mathbf{u}_{31,1}\ \nu_{31,2}\mathbf{u}_{32}\right]+\\ +\nu_{41,1}\mathbf{u}_{45}^T\left(\widetilde{\boldsymbol{\omega}}_{10}\mathbf{I}_{O,4}-\left[\widetilde{\boldsymbol{\omega}}_{10}\mathbf{I}_{O,4}\right]^T\right)\left[\nu_{41,1}\mathbf{u}_{45}\ \nu_{41,2}\mathbf{u}_{41,2}\right]\end{array}\right.\\ \left[\begin{array}{l}\mathbf{d}_{12}^T=\nu_{31,2}\mathbf{u}_{32}^T\left(\widetilde{\boldsymbol{\omega}}_{10}\mathbf{I}_{O,3}-\left[\widetilde{\boldsymbol{\omega}}_{10}\mathbf{I}_{O,3}\right]^T\right)\left[\nu_{31,1}\mathbf{u}_{31,1}\ \nu_{31,2}\mathbf{u}_{32}\right]+\\ +\nu_{41,2}\mathbf{u}_{41,2}^T\left(\widetilde{\boldsymbol{\omega}}_{10}\mathbf{I}_{O,4}-\left[\widetilde{\boldsymbol{\omega}}_{10}\mathbf{I}_{O,4}\right]^T\right)\left[\nu_{41,1}\mathbf{u}_{45}\ \nu_{41,2}\mathbf{u}_{41,2}\right]+\\ +\mathbf{u}_{51}^T\left(\widetilde{\boldsymbol{\omega}}_{10}\mathbf{I}_{O,5}-\left[\widetilde{\boldsymbol{\omega}}_{10}\mathbf{I}_{O,5}\right]^T\right)\left[\mathbf{0}\ \mathbf{u}_{51}\right]\end{array}\right.\end{array}\right. \tag{44c}$$

$$\left.\begin{array}{l}d_{0k}=\sum_{j=2,5}\nu_{j1,k}\left[m_j\left(G_j-O\right)\times{}^0\mathbf{a}_{O|1}+\mathbf{I}_{Oj}\dot{\boldsymbol{\omega}}_{10}+\boldsymbol{\omega}_{10}\times\left(\mathbf{I}_{Oj}\boldsymbol{\omega}_{10}\right)\right]\cdot\mathbf{u}_{j1,k}\\ \text{with}\quad k=1,2\end{array}\right\}$$

$$\Rightarrow\left\{\begin{array}{l}\left[\begin{array}{l}d_{01}=\left[m_2(G_2-O)\times{}^0\mathbf{a}_{O|1}+\mathbf{I}_{O,2}\dot{\boldsymbol{\omega}}_{10}+\boldsymbol{\omega}_{10}\times\left(\mathbf{I}_{O,2}\boldsymbol{\omega}_{10}\right)\right]\cdot\mathbf{u}_{21}+\\ +\nu_{31,1}\left[m_3(G_3-O)\times{}^0\mathbf{a}_{O|1}+\mathbf{I}_{O,3}\dot{\boldsymbol{\omega}}_{10}+\boldsymbol{\omega}_{10}\times\left(\mathbf{I}_{O,3}\boldsymbol{\omega}_{10}\right)\right]\cdot\mathbf{u}_{31,1}+\\ +\nu_{41,1}\left[m_4(G_4-O)\times{}^0\mathbf{a}_{O|1}+\mathbf{I}_{O,4}\dot{\boldsymbol{\omega}}_{10}+\boldsymbol{\omega}_{10}\times\left(\mathbf{I}_{O,4}\boldsymbol{\omega}_{10}\right)\right]\cdot\mathbf{u}_{45}\end{array}\right.\\ \left[\begin{array}{l}d_{02}=\nu_{31,2}\left[m_3(G_3-O)\times{}^0\mathbf{a}_{O|1}+\mathbf{I}_{O,3}\dot{\boldsymbol{\omega}}_{10}+\boldsymbol{\omega}_{10}\times\left(\mathbf{I}_{O,3}\boldsymbol{\omega}_{10}\right)\right]\cdot\mathbf{u}_{32}+\\ +\nu_{41,2}\left[m_4(G_4-O)\times{}^0\mathbf{a}_{O|1}+\mathbf{I}_{O,4}\dot{\boldsymbol{\omega}}_{10}+\boldsymbol{\omega}_{10}\times\left(\mathbf{I}_{O,4}\boldsymbol{\omega}_{10}\right)\right]\cdot\mathbf{u}_{41,2}+\\ +\left[m_5(G_5-O)\times{}^0\mathbf{a}_{O|1}+\mathbf{I}_{O,5}\dot{\boldsymbol{\omega}}_{10}+\boldsymbol{\omega}_{10}\times\left(\mathbf{I}_{O,5}\boldsymbol{\omega}_{10}\right)\right]\cdot\mathbf{u}_{51}\end{array}\right.\end{array}\right. \tag{44d}$$

By using the mass-distribution data reported in Table 1 and the mechanism motion data reported in Table 2 for the generalized coordinates, θ_{21} and θ_{51}, the above deduced model (Eq. 43) leads to compute the time histories of the generalized torques $\tau_1^{(i)}$ and $\tau_2^{(i)}$, where $i=1,2$ refers to the position analysis solution given by Eq. (39), shown in Fig. 12. In this case, the computed generalized torques equilibrate only the inertia forces due to the mechanism with fixed frame.

Moreover, by considering, during the mechanism motion, also the application to the links of the resultant moments, $\mathbf{M}_{O,j}^e$ for j=2, 3,

4, 5, reported in Table 3, the time histories of the generalized torques $\tau_1^{(i)}$ and $\tau_2^{(i)}$ shown in Fig. 13 are obtained. In this second case, the computed generalized torques equilibrate the inertia forces due to the mechanism motion with fixed frame and the external loads of Table 3.

Eventually, without external loads on the links, the combination of the mechanism motion and of the frame motion reported in Table 2 leads to compute the time histories of the generalized torques $\tau_1^{(i)}$ and $\tau_2^{(i)}$ shown in Fig. 14. In this third case, the computed generalized torques equilibrate the inertia forces due to the mechanism motion and to the frame motion, both reported in Table 2.

In Figs. 12, 13 and 14, the shown curves are cubic spline interpolations of 63 computed values of the generalized torques that are uniformly spaced in the time interval [0 2π] s, which covers one full cycle of oscillation of θ_{21} and θ_{51} (see Table 2).

4. Discussion

Matrix $\mathbf{B}(\mathbf{q})$ that appears in Eq. (31) is clearly the *generalized inertia matrix* [34] of the n-DOF spherical mechanism written through the IPA directions. In particular, the generic entry, b_{sk}, with $s, k = 1, \ldots, n$, of $\mathbf{B}(\mathbf{q})$ is expressible (see Eq. (29a)) by summing up terms that are quadratic in the VCs, $\nu_{ji,r}$, and in the components of the unit vectors, $\mathbf{u}_{ji,r}$, parallel to the IPAs, both referred to the single-DOF mechanisms generated from the n-DOF one. Also, it is worth stressing that the k-th diagonal entry, b_{kk}, coincides with the *equivalent moment of inertia* [28] of the k-th single-DOF spherical mechanism. Thus, the found expression of $\mathbf{B}(\mathbf{q})$ is interpretable as an extension to spherical multi-DOF mechanisms of the one found by Eksergian [43] for the equivalent moment of inertia of single-DOF mechanisms. This novel expression of $\mathbf{B}(\mathbf{q})$, which analytically relates the multi-DOF mechanism to the single-DOF ones it generates, is particularly useful to guide designers in deciding how to intervene for satisfying design requirements on the mechanism dynamics. Analogous considerations hold for the matrices $\mathbf{C}_k$ (see Eqs. (30) and (28b)) and their entries, $c_{sr,k}$ (Eq. (29b)).

The case study, illustrated in section 3, visually highlights that the PKA computations must not be repeated when the motion data and/or the external load data change. Indeed, the diagrams of Figs. 7−11 are the same for the three dynamic analyses reported in section 3.2. As a consequence, if the mechanism geometry does not change the computation burden is consistently reduced, which makes the proposed formulation usable even in online control applications. In particular, the same diagrams provide an example of how the PKA database could be built.

In the case study, the PKA database has been replaced by the analytic relationships. When such relationships are available, this is always possible; nevertheless, if such expressions are cumbersome, the convenience of using them instead of a database must be carefully evaluated especially in online control applications. For instance, in the case study of Section 3, this author exploited the symbolic calculus as implemented in the "Symbolic Math Toolbox" of Matlab; this approach was easy to implement (it was sufficient to type the formulas reported in Section 3 inside a Matlab script) and guaranteed the correctness of the deduced formulas, which could be even not displayed, but brought to define a number of nested "*anonymous function handles*" (see the online "Matlab tutorial" (https://it.mathworks.com/help/matlab/matlab_prog/anonymous-functions.html) for the definition) that made the numerical computation inefficient.

An average data-retrieving time is 10^{-7}s (which is a realistic value for the storage devices available today) to get one value in double-precision floating-point format (64bit) from the PKA database. Consequently, retrieving all the entries of the $n\times n$ matrices $\mathbf{B}$ and $\mathbf{C}_k$, k=1, …, n, for an assigned $\mathbf{q}$ value (i.e., mechanism configuration) would require $n^2(1+n)\times 10^{-7}$ s. In addition, retrieving all the other data necessary to compute the remaining terms appearing in the k-th Eq. (30) would require $l(4n+3)\times 10^{-7}$ s. Moreover, in the k-th Eq. (30), the computation of the first two terms (i.e., $\mathbf{b}_k^T\ddot{\mathbf{q}} + \dot{\mathbf{q}}^T\mathbf{C}_k\dot{\mathbf{q}}$) requires $n(2+n)$ multiplications and n^2 additions. The computation of $Q_{k,e}$ requires $4l$ multiplications and $2l$ additions. The computation of the third term (i.e., $\mathbf{d}_{1k}^T\dot{\mathbf{q}}$) requires $n+l(4n+36)$ multiplications and $l(25+2n)-1$ additions and, finally, the computation of the fourth term (i.e., d_{0k}) requires $43l$ multiplications and $29l-1$ additions. Therefore, computing τ_k through Eq. (30) requires $n(3+n)+l(4n+83)$ multiplications and $n^2+2[l(28+n)-1]$ additions, which yields a total of $n(3+2n)+l(6n+139)-2$ FLOP (*FLoating-point OPerations*). An old Pentium 4 with a 1.3 GHz of clock rate, which is dated back on 2000, is able to execute $2\times 1.3\times 10^9$ FLOP/s. With this computation rate, all the τ_k are computable in $\{l[n(3+2n)+l(6n+139)-2]/260+[\,n^2(1+n)+l(4n+3)]\}\times 10^{-7}$ s, which, for the case study of section 3 with n=2 and l=5, yields 8.17×10^{-6} s. Since real-time control requires computation times of few milliseconds, this value confirms that the proposed algorithm is applicable in online control applications.

In real-time control the adopted algorithm, over being fast enough, must be able to provide sufficient pieces of information to the control system for avoiding the occurrence of singular configurations [25,32] during the online path planning. Singular configurations (singularities) are configurations where the mechanism locally either acquires additional infinitesimal DOFs (uncertainty configurations), or reduces its infinitesimal DOFs (stationary configurations). Such configurations [25,32] must be avoided during the mechanism operation since they make critical static and kinematic conditions arise that could also cause the breakdown of the

Table 2
Motion data of the generalized coordinates, θ_{21} and θ_{51}, and of the frame (t is the time; the vector components of $\boldsymbol{\omega}_{10}$ and ${}^0\mathbf{a}_{O|1}$ are measured in $Ox_1y_1z_1$).

$\theta_{21}(t)$ [rad]	$\theta_{51}(t)$ [rad]	$\boldsymbol{\omega}_{10}(t)$ [rad/s]	${}^0\mathbf{a}_{O\|1}(t)$ [m/s^2]
sin$t$	sin$t$	$\begin{pmatrix}1\\0\\0\end{pmatrix}\sin(10t)$	$\begin{pmatrix}0\\0\\1\end{pmatrix}\cos(5t)$

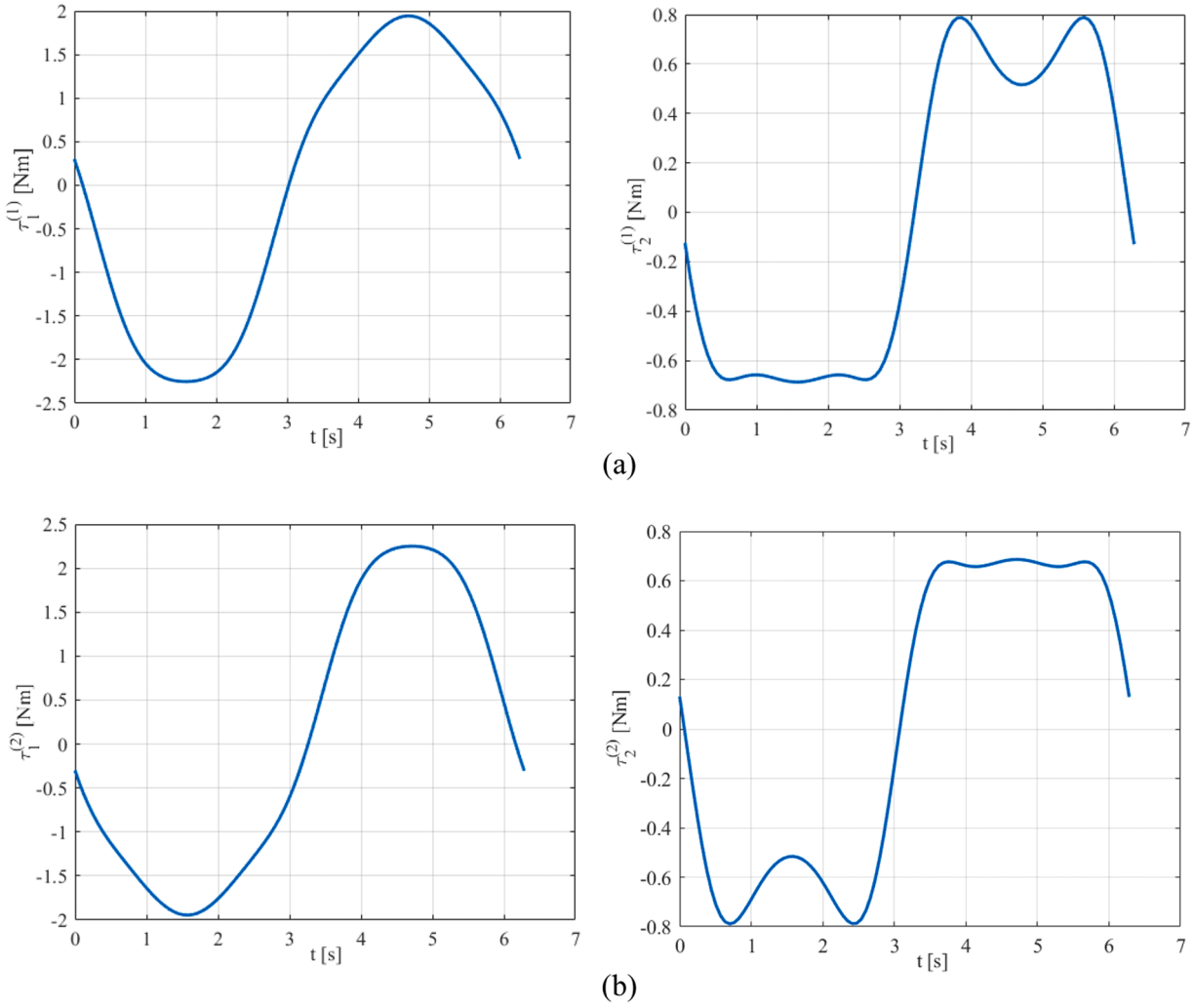

Fig. 12. Computed time histories of the generalized torques $\tau_1^{(i)}$ and $\tau_2^{(i)}$ for $i = 1$ (a) and $i = 2$ (b), where $i = 1, 2$ refers to the position analysis solution given by Eq. (39), in the case of mechanism motion with fixed frame detailed in Table 2 through $\theta_{21}(t)$ and $\theta_{51}(t)$ (the shown curves are cubic spline interpolations of 63 computed values of the generalized torques that are uniformly spaced in the time interval [0 2π] s).

Table 3
Active-load data used to compute the generalized torques shown in Fig. 13 (the vector components are all measured in the reference system fixed to the link they are applied to).

$\mathbf{M}^e_{O,2}$ [N m]	$\mathbf{M}^e_{O,3}$ [N m]	$\mathbf{M}^e_{O,4}$ [N m]	$\mathbf{M}^e_{O,5}$ [N m]
$\begin{pmatrix} 0 \\ 0.5 \\ 0.5 \end{pmatrix}$	$\begin{pmatrix} 0 \\ 1 \\ 3 \end{pmatrix}$	$\begin{pmatrix} 0 \\ 4 \\ 1 \end{pmatrix}$	$\begin{pmatrix} 0 \\ 0.5 \\ 0.5 \end{pmatrix}$

machine. The proposed formulation uses VCs and VCs are a primary tool for revealing the occurrence of singularities [25,32]; consequently, it is able to provide all the necessary pieces of information to the control system for avoiding singularities. In particular, VCs are mapped during the PKA (see Figs. 2,8–11) and these mappings allow the identification of all the joint-space's regions that are too close to singularities. During design, these VC mappings can be used either to define the control algorithm so that the machine always works in safe regions of its workspace or to modify the machine geometry to get better VC mappings that do not contain singularities in the workspace regions where the machine must work according to the design requirements.

Any phenomenon (e.g., clearances and/or friction in the joints, link flexibility, etc.) that can be modelled either by modifying the mechanism type or by applying forces (even depending on the mechanism configuration) or by implementing both the previous actions can be modelled into the proposed formulation provided that, when the mechanism type is modified, it remains a spherical

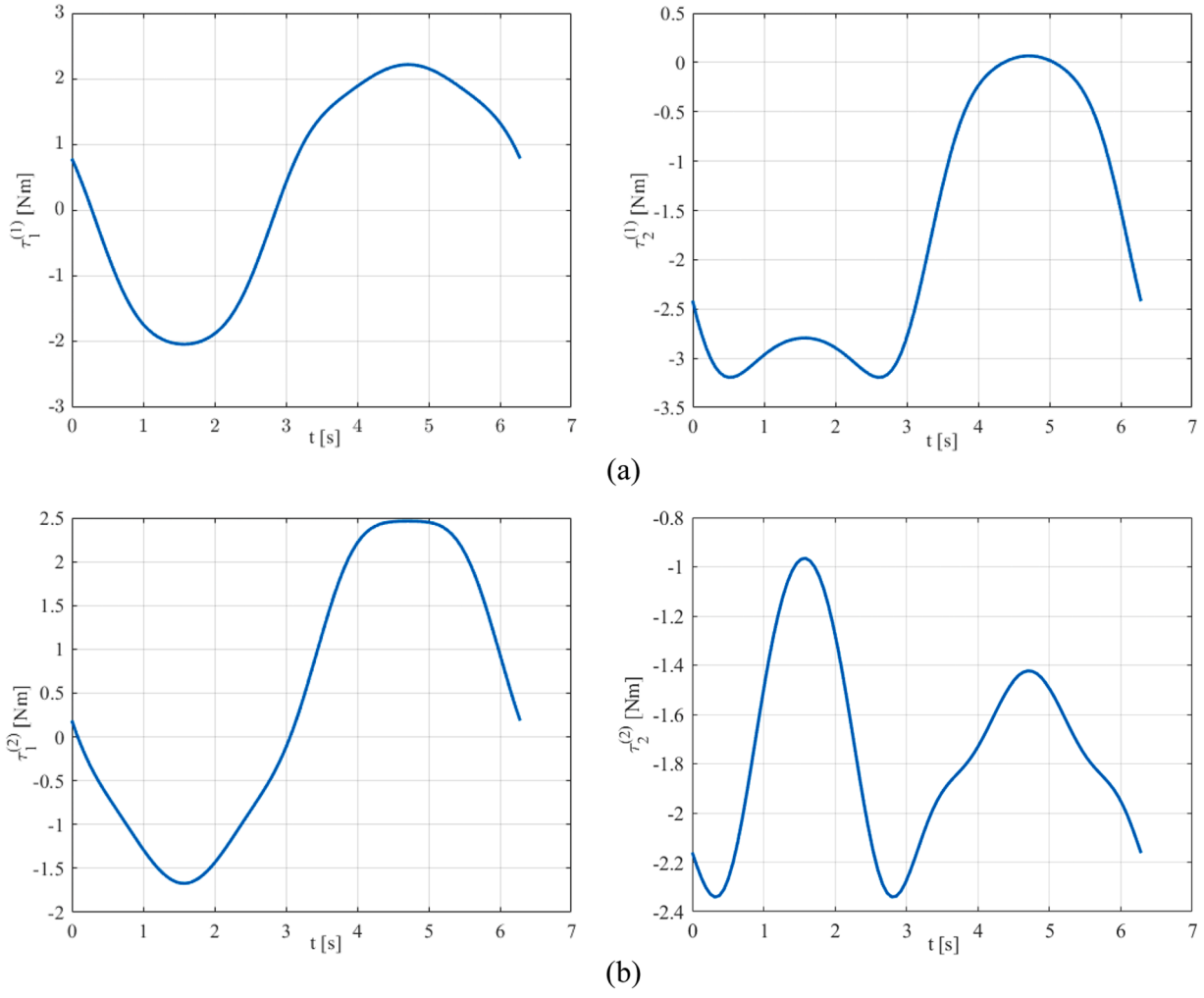

Fig. 13. Computed time histories of the generalized torques $\tau_1^{(i)}$ and $\tau_2^{(i)}$ for $i = 1$ (a) and $i = 2$ (b), where $i = 1, 2$ refers to the position analysis solution given by Eq. (39), in the case of mechanism motion with fixed frame as detailed in Table 2 through $\theta_{21}(t)$ and $\theta_{51}(t)$ and external loads applied to the link as detailed in Table 3 (the shown curves are cubic spline interpolations of 63 computed values of the generalized torques that are uniformly spaced in the time interval [0 2π] s).

mechanism. In particular, the mechanism changes both in geometry and in type generate a new equation system (Eq. (27)); whereas, the new force elements just enter into the computation of the terms Q_k, for k=1, …, n, (Eq. (28a)). In short, the only limitation on the introduction of non-idealities in the links and in the joints is that they must keep the motion spherical. Such a limitation is not so tight since it is similar to the one that planar dynamics formulations must satisfy.

In the literature, most of the dynamic models proposed for spherical mechanisms [17–20,44–50] either focus on specific spherical architectures [17,19,45,46,49] or address specific issues (e.g., accuracy [20], control [48]) by using different dynamics' formulations (Newton-Euler formulation [19], Lagrangian formulation [44,46], Gibbs-Appell method [18], Virtual Work principle [48,49], Screw theory [50], etc.). Only few works propose general formulations [18,44,50] for multi-DOF spherical mechanisms' dynamics. These works mainly adapt models conceived for spatial mechanisms to spherical ones and never take into account a possible frame motion. Differently, the general formulation presented here highlights specific features of spherical dynamics such as the connection between the IPA locations and the dynamic performances and how the dynamics of a multi-DOF spherical mechanism is related to those of the single-DOF mechanisms it generates. Also, it is able to take into account a general motion of the frame. These specific features make the proposed formulation more suitable than others to support designers in their choices when they have to match dynamic requirements. Eventually, the deduction of the proposed dynamic model has brought to write the explicit expression of the generalized inertia matrix as a function of the VCs. Such an explicit expression, which is a general form applicable to multi-DOF spherical mechanisms of the one found by Eksergian [43] for single-DOF mechanisms, is presented for the first time.

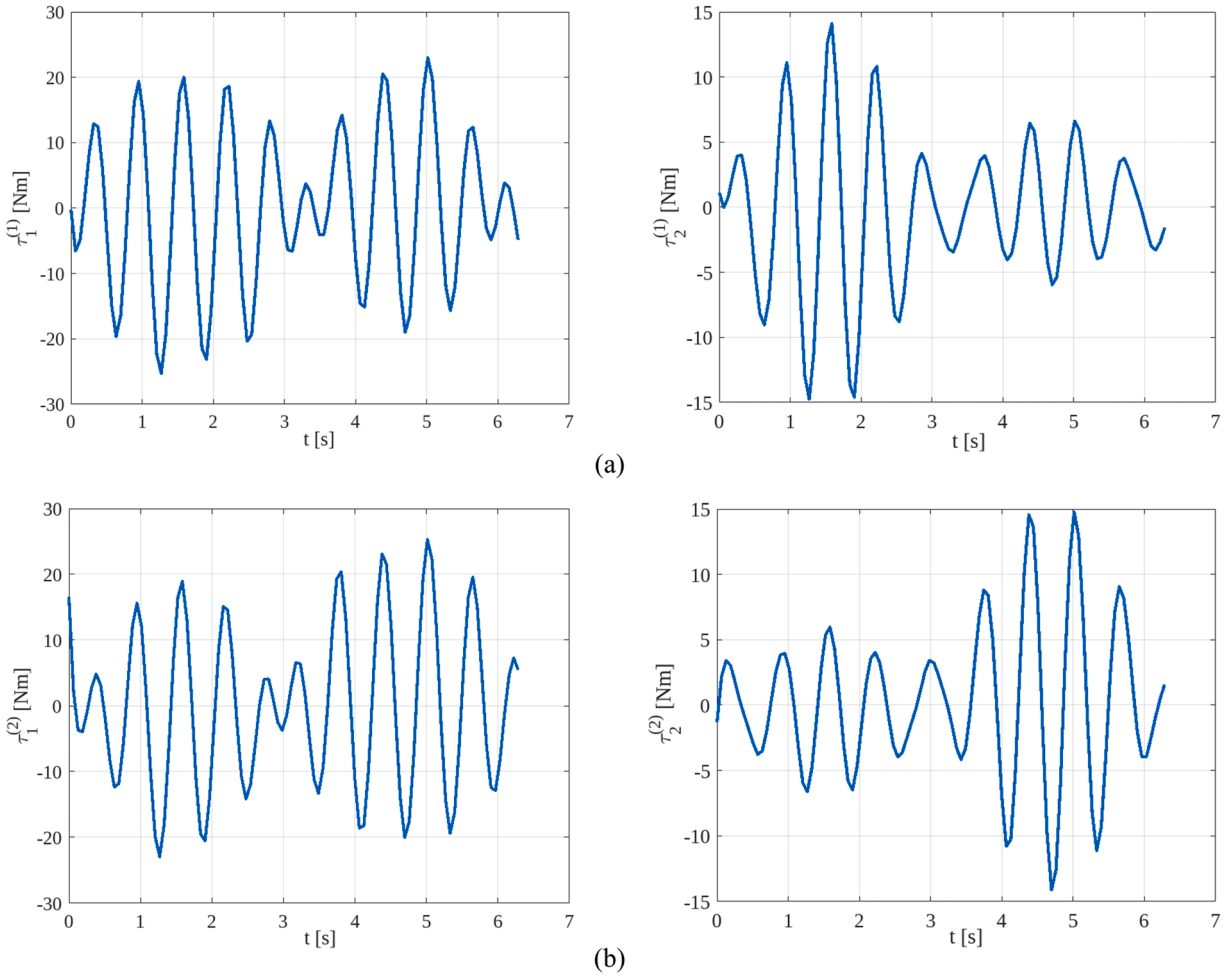

Fig. 14. Computed time histories of the generalized torques $\tau_1^{(i)}$ and $\tau_2^{(i)}$ for $i = 1$ (a) and $i = 2$ (b), where $i = 1, 2$ refers to the position analysis solution given by Eq. (39), in the case of mechanism and frame motion as detailed in Table 2 through $\theta_{21}(t)$, $\theta_{51}(t)$, $\boldsymbol{\omega}_{10}(t)$ and ${}^0\mathbf{a}_{O|1}(t)$ (the shown curves are cubic spline interpolations of 63 computed values of the generalized torques that are uniformly spaced in the time interval [0 2π] s).

5. Conclusions

Starting from the D'Alembert's principle and the relationships between the instantaneous pole axes (IPAs) of a multi-DOF spherical mechanism and the IPAs of the single-DOF spherical mechanisms it generates, a novel general dynamic model for multi-DOF spherical mechanisms has been deduced. This model fully highlights the role played by the instantaneous pole axes (IPAs) locations in the dynamic performances of these mechanisms and it is more prone than others to support designers that have to match specific requirement on such performances. Moreover, it can take into account also a possible motion of the frame.

In particular, the velocity coefficients (VCs) of the single-DOF spherical mechanisms generated from the multi-DOF one by locking all the generalized coordinates but one have been expressed through unit vectors parallel to the IPAs and, then, used to write all the terms appearing in D'Alembert's principle. How to use the deduced model in the solution of the inverse and the direct dynamics problems has been detailed through ad hoc algorithms that need a common preliminary kinematic analysis, which can be done only once if the mechanism geometry does not change. This feature makes the proposed algorithms fast enough for them to be used in real-time applications.

The deduction of the model has brought to write the explicit expression of the generalized inertia matrix as a function of the VCs of the single-DOF spherical mechanisms generated from the multi-DOF one. Such an explicit expression, which is a general form applicable to multi-DOF spherical mechanisms of the one found by Eksergian for single-DOF mechanisms, is presented for the first time.

Eventually, a relevant case study has been addressed through the proposed novel formulation to show its effectiveness in solving a real dynamic problem.

CRediT authorship contribution statement

Raffaele Di Gregorio: Writing – review & editing, Writing – original draft, Visualization, Validation, Supervision, Software, Resources, Project administration, Methodology, Investigation, Funding acquisition, Formal analysis, Data curation, Conceptualization.

Declaration of competing interest

The authors declare that they have no known competing financial interests or personal relationships that could have appeared to influence the work reported in this paper.

Acknowledgements

This work has been developed at the Laboratory of Mechatronics and Virtual Prototyping (LaMaViP) of Ferrara Technopole, supported by FAR2023 UNIFE funds.

Data availability

No data was used for the research described in the article.

References

[1] Chiang C. H., Kinematics of spherical mechanisms, Krieger Publishing Company, Malabar, Florida, USA, 2000.
[2] T.A. Hess-Coelho, A redundant parallel spherical mechanism for robotic wrist applications, ASME J. Mech. Des 129 (8) (August 2007) 891–895, https://doi.org/10.1115/1.2735645.
[3] M. Arredondo-Soto, E. Cuan-Urquizo, A. Gómez-Espinosa, A. Roman-Flores, P.D. Urbina-Coronado, M. Jimenez-Martinez, The compliant version of the 3-RRR spherical parallel mechanism known as "agile-eye": kinetostatic analysis and parasitic displacement evaluation, Mech. Mach. Theory. 180 (2023) 105160, https://doi.org/10.1016/j.mechmachtheory.2022.105160.
[4] O. Acar, H. Sağlam, Z. Şaka, Evaluation of grasp capability of a gripper driven by optimal spherical mechanism, Mech. Mach. Theory. 166 (2021) 104486, https://doi.org/10.1016/j.mechmachtheory.2021.104486.
[5] N.M. Bajaj, A.J. Spiers, A.M. Dollar, State of the art in artificial wrists: a review of prosthetic and robotic wrist design, IEEE Trans. Robot. 35 (1) (February 2019) 261–277, https://doi.org/10.1109/TRO.2018.2865890.
[6] T. Essomba, W.-H. Wang, Design of a spherical parallel mechanism with controllable center of rotation using a spherical reconfiguration linkage, Mech. Mach. Theory. 199 (2024) 105672, https://doi.org/10.1016/j.mechmachtheory.2024.105672.
[7] S. Mghames, M.G. Catalano, A. Bicchi, G. Grioli, A spherical active joint for humanoids and humans, IEEE Robot. Autom. Lett. 4 (2) (April 2019) 838–845, https://doi.org/10.1109/LRA.2019.2893423.
[8] H. Fan, G. Wei, L. Ren, Prosthetic and robotic wrists comparing with the intelligently evolved human wrist: a review, Robotica 40 (11) (2022) 4169–4191, https://doi.org/10.1017/S0263574722000856.
[9] J. Zhang, C. Liu, T. Liu, K. Qi, J. Niu, S. Guo, Module combination based configuration synthesis and kinematic analysis of generalized spherical parallel mechanism for ankle rehabilitation, Mech. Mach. Theory. 166 (2021) 104436, https://doi.org/10.1016/j.mechmachtheory.2021.104436.
[10] J.M. Hervé, Uncoupled actuation of pan-tilt wrists, IEEE Trans. Robot. 22 (1) (Feb. 2006) 56–64, https://doi.org/10.1109/TRO.2005.858859.
[11] X. Kong, Forward displacement analysis of a 2-DOF RR-RRR-RRR spherical parallel manipulator, in: Procs. of 2010 IEEE/ASME international conference on mechatronic and embedded systems and applications, Qingdao, China, 2010, pp. 446–451, https://doi.org/10.1109/MESA.2010.5551993.
[12] W. Li, J. Angeles, M. Valášek, Contributions to the kinematics of pointing, Mech. Mach. Theory. 108 (2017) 97–109, https://doi.org/10.1016/j.mechmachtheory.2016.10.018.
[13] W. Wang, X. Li, P. Yan, H. Huang, B. Li, Design of self-deployable origami utilizing rigid-elastic coupling spherical mechanism, Mech. Mach. Theory. 201 (2024) 105749, https://doi.org/10.1016/j.mechmachtheory.2024.105749.
[14] Y. Chen, X. Zhang, Y. Huang, Y. Wu, J. Ota, Error modeling and analysis of a spherical parallel mechanism with a multiloop circuit incremental method, Mech. Mach. Theory. 191 (2024) 105523, https://doi.org/10.1016/j.mechmachtheory.2023.105523.
[15] X. Kong, C.M. Gosselin, A formula that produces a unique solution to the forward displacement analysis of a quadratic spherical parallel manipulator: the agile eye, ASME J. Mech. Robot. 2 (4) (November 2010) 044501, https://doi.org/10.1115/1.4002077.
[16] G. Mullineux, Atlas of spherical four-bar mechanisms, Mech. Mach. Theory. 46 (11) (2011) 1811–1823, https://doi.org/10.1016/j.mechmachtheory.2011.06.001.
[17] E. Kayacan, Z.Y. Bayraktaroglu, W. Saeys, Modeling and control of a spherical rolling robot: a decoupled dynamics approach, Robotica 30 (4) (2012) 671–680, https://doi.org/10.1017/S0263574711000956.
[18] E. Abedloo, A. Molaei, H.D. Taghirad, Closed-form dynamic formulation of spherical parallel manipulators by Gibbs-Appell method, in: 2014 Second RSI/ISM International Conference on Robotics and Mechatronics (ICRoM), Tehran, Iran, 2014, pp. 576–581, https://doi.org/10.1109/ICRoM.2014.6990964.
[19] A. Arian, B. Danaei, M.T. Masouleh, Kinematics and dynamics analysis of a 2-DOF spherical parallel robot, in: 2016 4th International Conference on Robotics and Mechatronics (ICROM), Tehran, Iran, 2016, pp. 154–159, https://doi.org/10.1109/ICRoM.2016.7886838.
[20] D.T. Vo, S. Kheylo, V.Q. Nguyen, Kinematic and dynamic accuracy of spherical mechanisms, Mech. Sci. 13 (2022) 23–30, https://doi.org/10.5194/ms-13-23-2022.
[21] S. Kheylo, V. Glazunov, Kinematics, dynamics, control and accuracy of spherical parallel robot, in: M. Ceccarelli, V. Glazunov (Eds.), Advances on Theory and Practice of Robots and Manipulators. Mechanisms and Machine Science, Advances on Theory and Practice of Robots and Manipulators. Mechanisms and Machine Science, 22, Springer, Cham, 2014, https://doi.org/10.1007/978-3-319-07058-2_15.
[22] T.J. Furlong, J.M. Vance, P.M. Larochelle, Spherical mechanism synthesis in virtual reality, ASME. *J. Mech. Des.* 121 (4) (1999) 515–520, https://doi.org/10.1115/1.2829491. December.
[23] A. Diouf, B. Belzile, M. Saad, D. St-Onge, Spherical rolling robots—design, modeling, and control: a systematic literature review, Rob Aut. Syst. 175 (2024) 104657, https://doi.org/10.1016/j.robot.2024.104657.
[24] H. Nigatu, L. Jihao, G. Shi, G. Lu, H. Dong, Unveiling the complete variant of spherical robots, arXiv (2024), https://doi.org/10.48550/arXiv.2403.03505 arXiv:2403.03505v1[cs.RO].
[25] R. Di Gregorio, Analytic and geometric technique for the singularity analysis of multi-degree-of-freedom spherical mechanisms, ASME J. Mech. Robot. 7 (3) (2015) 031008, https://doi.org/10.1115/1.4028625 (9 pages).
[26] R. Di Gregorio, A general algorithm for analytically determining all the instantaneous pole axis locations in single-DOF spherical mechanisms, Proc. IMechE C: J. Mech. Eng. Sci. 225 (9) (2011) 2062–2075, https://doi.org/10.1177/0954406211404894.

[27] J.I. Valderrama-Rodríguez, J.M. Rico, J.J. Cervantes-Sánchez, A screw theory approach to compute instantaneous rotation axes of indeterminate spherical linkages, Mech. Based Des. Struct. Mach. 50 (8) (2022) 2836–2876, https://doi.org/10.1080/15397734.2020.1787841.
[28] R. Di Gregorio, Dynamic model of single-DOF spherical mechanisms based on instantaneous pole axes and Eksergian's equation, Mech. Mach. Theory. 200 (2024) 105720, https://doi.org/10.1016/j.mechmachtheory.2024.105720.
[29] Pars L. A., A treatise on analytical dynamics, Heinemann, London, UK, 1965.
[30] Di Gregorio, R., Kinematic analysis of multi-DOF planar mechanisms via velocity-coefficient vectors and acceleration-coefficient jacobians, mechanism and Machine theory, 142 (2019): 103617. doi: 10.1016/j.mechmachtheory.2019.103617.
[31] Doughty S., Mechanics of machines, 2nd Ed. Ver. 2.1, Doughty Samuel's profile on Academia.edu: Dubuque, IA, USA, 2019 (self-produced by the author and freely downloadable).
[32] R. Di Gregorio, Analytical method for the singularity analysis and exhaustive enumeration of the singularity conditions in single-degree-of-freedom spherical mechanisms, Proc. IMechE C: J. Mech. Eng. Sci. 227 (8) (2013) 1830–1840, https://doi.org/10.1177/0954406212469328.
[33] Ardema M.D., Newton-euler dynamics, Springer, New York, NY, 2005.
[34] Angeles J., Fundamentals of robotic mechanical systems, Springer, New York, NY, 2014.
[35] Fröberg C.-E., Introduction to numerical analysis, 2nd Ed., Addison-Wesley Publishing Company, Reading, Massachusetts (USA), 1969.
[36] M. Ouerfelli, V. Kumar, Optimization of a spherical five-bar parallel drive linkage, ASME *J. Mech. Des.* 116 (1) (March 1994) 166–173, https://doi.org/10.1115/1.2919341.
[37] D. Kohli, A. Khonji, Grashof-type rotatability criteria of spherical five-bar linkages, ASME. *J. Mech. Des.* 116 (1) (March 1994) 99–104, https://doi.org/10.1115/1.2919384.
[38] E. Emmanouil, G. Wei, J.S. Dai, Spherical trigonometry constrained kinematics for a dexterous robotic hand with an articulated palm, Robotica 34 (12) (2016) 2788–2805, https://doi.org/10.1017/S0263574715000399.
[39] Y. Zheng, W. Guo, Y. Xie, Dynamic modeling of spherical 5R parallel mechanism for spherical plain bearing running-in equipment, in: X. Zhang, N. Wang, Y. Huang (Eds.), Mechanism and Machine Science. ASIAN MMS & CCMMS 2016, Springer, Singapore, 2016, p. 2017, https://doi.org/10.1007/978-981-10-2875-5_89. Lecture Notes in Electrical Engineering, Vol. 408.
[40] P. Boscariol, A. Gasparetto, L. Scalera, R. Vidoni, Efficient closed-form solution of the kinematics of a tunnel digging machine, ASME. J. Mech. Robot. 9 (3) (2017) 031001, https://doi.org/10.1115/1.4035797. June.
[41] T. Essomba, L.N. Vu, Kinematic analysis of a new five-bar spherical decoupled mechanism with two-degrees of freedom remote center of motion, Mech. Mach. Theory. 119 (2018) 184–197, https://doi.org/10.1016/j.mechmachtheory.2017.09.010.
[42] W. Zhang, Z. Liu, J. Sun, B. Sun, Path synthesis of a spherical five-bar mechanism based on a numerical atlas method, J Braz. Soc. Mech. Sci. Eng. 44 (2022) 554, https://doi.org/10.1007/s40430-022-03860-w (16 pages).
[43] Eksergian, R., Dynamical analysis of machines, Ph.D. dissertation, Clark University, Worcester, MA, 1928. (15 articles published on J. of the Franklin Institute, Voll. 209–211 (1930–1931), report an extended version of this thesis).
[44] R. Di Gregorio, V. Parenti-Castelli, Dynamics of a class of parallel wrists, ASME J. Mech. Des. 126 (3) (May 2004) 436–441, https://doi.org/10.1115/1.1737382.
[45] B. Danaei, A. Arian, M.T. Masouleh, A. Kalhor, Dynamic modeling and base inertial parameters determination of a 2-DOF spherical parallel mechanism, Multibody Syst. Dyn. 41 (4) (June 2017) 367–390, https://doi.org/10.1007/s11044-017-9578-3.
[46] X. Li, S. Bai, O. Madsen, Dynamic modeling and trajectory tracking control of an electromagnetic direct driven spherical motion generator, Robot. Comput. Integr. Manuf. 59 (2019) 201–212, https://doi.org/10.1016/j.rcim.2019.04.009.
[47] S. Bai, X. Li, J. Angeles, A review of spherical motion generation using either spherical parallel manipulators or spherical motors, Mech. Mach. Theory. 140 (2019) 377–388, https://doi.org/10.1016/j.mechmachtheory.2019.06.012.
[48] Hassania A., Bataleblua A., Khalilpoura S. A., Taghirada H. D., Cardou P., Dynamic models of spherical parallel robots for model-based control schemes, Cornell University, arXiv:2110.00491v1 [cs.RO], October 2021. doi: 10.48550/arXiv.2110.00491.
[49] S. Staicu, Recursive modelling in dynamics of agile wrist spherical parallel robot, Robot. Comput. Integr. Manuf. 25 (2) (2009) 409–416, https://doi.org/10.1016/j.rcim.2008.02.001.
[50] J. Gallardo, J.M. Rico, A. Frisoli, D. Checcacci, M. Bergamasco, Dynamics of parallel manipulators by means of screw theory, Mech. Mach. Theory. 38 (11) (2003) 1113–1131, https://doi.org/10.1016/S0094-114X(03)00054-5.